in each group).[33,34] Cells were trypsinized and seeded at a density of approximately 5000 cells/well in 96-well cell culture plates in 100 μL of culture medium with 10% FBS. After 24 h, the medium was refreshed with the culture medium using 1% FBS containing growth factors, PRP, and PPP at the indicated concentrations (3%, 10%, 30%). After 48 h, the medium was removed and washed with PBS, then refreshed with fresh medium containing MTS reagent (100 μL medium with 1% FBS plus 20 μL MTS reagent/well). The optical density was measured at 490 nm using an automatic microplate reader after 1.5 h of further incubation at 37°C in a humidified atmosphere of 5% CO_2. The percentage viability of each well was calculated.

Cell proliferation ELISA and 5-bromo-2'-deoxyuridine assay. Meniscal cell proliferation was determined using a colorimetric immunoassay, based on the measurement of 5-bromo-2'-deoxyuridine (BrdU) incorporated in newly synthesized cellular deoxyribonucleic acid (DNA) ($n = 5$ in each group).[35,36] The cells were seeded, and the medium was refreshed using the same method as MTS assay for 48 h, after which BrdU was added to a final concentration of 10 μM. After incubation for 4 h, DNA synthesis was assayed using the Cell Proliferation ELISA, BrdU kit (Roche Molecular Biochemicals, Penzberg, Germany) according to the manufacturer's instructions.

Assessment of ECM formation. Quantitative dye-binding assays and Alcian blue-binding assays were performed to measure the amounts of ECM and sulphated glycosaminoglycans (sGAGs) in the culture medium ($n = 4$ in each group).[37] There was no interference from proteins or nucleic acids using this method, and this assay could detect sGAGs in blood samples.[37] Briefly, after seeding the meniscal cells at a density of approximately 10,000 cells/well in 96-well cell culture plates, the medium was refreshed the next day with a culture medium with 1% FBS containing 10% PRP. On days 2, 4, 6, and 8, the supernatants were collected and replaced with a new culture medium containing 10% PRP. The gathered supernatants were assayed using Alcian blue-binding assays (Wieslab AB, Ideon, Sweden) according to the manufacturer's instructions. Culture medium containing 10% PPP was also collected and assayed.

Gene expression analysis. To investigate the transcriptional expression of meniscal cell-related genes, we used real-time quantitative reverse transcriptase polymerase chain reaction (PCR) ($n = 5$ in each group) according to the manufacturer's instructions (Takara Bio, Shiga, Japan). Briefly, after culturing meniscal cells for 48 h, total ribonucleic acid (RNA) was isolated using RNeasy Mini Kit (Qiagen, Valencia, CA). Reverse transcription of RNA into complementary DNA (cDNA) was performed by incubating approximately 1 μg of RNA using oligo (dT) primer, deoxyribonucleotide triphosphate, 10×PCR buffer, magnesium chloride, RNase inhibitor, and Mulv Reverse Transcriptase (all from Applied Biosystems, Foster City, CA). The converted cDNA (2 μL) samples were amplified in triplicate using real-time PCR (ABI PRISM 7700) in a final volume of 50 μL using SYBR Green Master Mix reagent at a final concentration of 1×(Applied Biosystems). The primer pairs of rabbit-specific genes were obtained using a previously reported method[38] and were designed by the manufacturer (Takara Bio) according to the published sequences available in GenBank (Table 1). Levels of transcripts for 18S ribosomal RNA proved to be stable and were therefore elected as a reference gene. Melting curve analysis was performed to ensure that only a single product was amplified using Dissociation Curves software (Applied Biosystems). Specificity of the reactions was confirmed using 2.5% agarose gel electrophoresis. Results were obtained using sequence detection software (ABI Prism 7700) and evaluated using Microsoft Excel (Microsoft Corp., Redmond, WA).

In vivo *study*

Preparation of gelatin hydrogels incorporating PRP. Gelatin hydrogels were prepared using chemical cross-linking

TABLE 1.

Gene	*Sequences*	*GeneBank accession no.*
Col 1	Sense: 5'-ATGGATGAGGAAACTGGCAACT-3' Antisense:5'-GCCATCGACAAGAACAGTGTAAGT-3'	D49399
Aggrecan	Sense: 5'-TCTACCGCTGTGAGGTGATGC-3' Antisense: 5'-TTCACCACGACCTCCAAGG-3'	L38480
Biglycan	Sense: 5'-AGGATCTGCTCCGATACTCCAA-3' Antisense: 5'-CAGGCTCCCGTTCTCAATCA-3'	AF020290
Decorin	Sense: 5'-CTGGACAAAGTGCCCAAGGA-3' Antisense: 5'-TGACGAGGATCAATGCGTGAA-3'	U03394
18S	Sense: 5'-CGGACACGGACAGGATTGAC-3' Antisense: 5'-CCAGACAAATCGCTCCACCA-3'	X06778

of aqueous gelatin solution with glutaraldehyde (GA; Wako Pure Chemical Industries, Osaka, Japan) according to a previously reported method.[31,32,39–41] The hydrogels were designed to biodegrade some of the individual growth factors for an average of approximately 2 weeks in *in vivo* conditions.[32,42] Briefly, gelatin with an isoelectric point of 5.0 (Nitta Gelatin, Osaka, Japan) was prepared as an acidic gelatin. After mixing 400 μL of aqueous GA (Wako Pure Chemical Industries) solution (25 wt%) with 80 mL of aqueous gelatin solution (5 wt%) preheated at 40°C, the mixed aqueous solution was cast into balance dishes and left for 12 h at 4°C to allow for chemical cross-linking of gelatin. The resulting hydrogel sheets were placed in 100 mM glycine aqueous solution and then agitated at 37°C for 1 h to block the residual aldehyde groups of unreacted GA. The cross-linking hydrogel sheets were thoroughly washed with double-distilled water, freeze-dried, and sterilized with ethylene oxide gas. The water content of gelatin hydrogel was 95 wt% when calculated from the hydrogel weight in the wet and dry state. The gelatin hydrogel sheets were cut into small squares (2×2 mm).

PRP (30 μL) was added by drops onto the freeze-dried gelatin hydrogel squares and left for 1 h at 37°C to allow it to impregnate the hydrogel. Similarly, empty gelatin hydrogel and gelatin hydrogel incorporating PPP were prepared as controls, in addition to using PPP and PBS.

Animal experiments. Eighteen skeletally mature female Japanese white rabbits (Kitayama Labs) with a mean weight of 3.1 kg (2.8 ± 3.3 kg) were used in this study. Surgical procedures were performed according to a previously reported method.[43–45] Briefly, after general anesthesia was administered, the rabbits were placed in the supine position and surgeries were performed on the bilateral knees. In each rabbit, the limbs were disinfected, and 5 mL of 1% lidocaine was injected subcutaneously, where the incision was to be made. A medial parapatellar approach was used to expose the knee joint, and the patella was everted. The knee was flexed to the maximum, and a 1.5-mm-diameter full-thickness circular defect was produced in the anterior portion of the inner two-thirds avascular zone of the medial meniscus using a biopsy punch (Kai Medical, Gifu, Japan). The defects were divided into 3 groups according to treatment as follows: Group A, defects were filled with gelatin hydrogel with PRP; Group B, defects were filled with gelatin hydrogel with PPP; Group C, defects were filled with gelatin hydrogel with PBS. Joint capsule and skin were sutured as separate layers in all groups. After surgery, all rabbits were returned to their cages and allowed to move freely without joint immobilization. Four, 8, and 12 weeks postoperatively, rabbits were euthanized with an intravenous injection of a fatal dose of pentobarbital sodium, and the operated meniscus was taken from the knee joint and prepared for histological evaluation ($n = 4$ in each group and at each time point).

Histological examination. The specimens were fixed in 4% paraformaldehyde in 0.1 M phosphate buffer solution for 4 h and embedded in paraffin wax. Each specimen was cut into slices, 7 μm thick, along the radial plane. For histological analysis, the section was stained with hematoxylin and eosin staining and Safranin-O fast green staining. The reparative tissue was evaluated using original semi-quantitative scoring (Table 2) using three different observers blind to treatment. Assessment points were divided into 3 as follows: 1) reparative tissue with bonding, assessing whether the reparative tissues had bonded with the surrounded normal meniscus tissues; 2) existence of fibrochondrocytes, and 3) stainability with Safranin-O. The total attainable score was 6 points, 2 for each category. The points were calculated and evaluated statistically and histologically for each specimen.

Statistical analysis

Data obtained were statistically analyzed using analysis of variance. A value of $p < 0.05$ was regarded as statistically significant.

RESULTS

In vitro *study*

Assessment of the prepared PRP. The mean number of counted thrombocytes in the peripheral blood was 21.33 $\times 10^4$/μL. The mean PRP platelet count was 104.45$\times 10^4$/μL. The mean PPP platelet count was 1.38$\times 10^4$/μL. The concentration of thrombocytes in PRP increased 4.89-fold according to the mechanical count ($p < 0.005$).

Analysis of growth factor concentrations in PRP samples and PPP samples using ELISA revealed that levels of growth factors were significantly higher in PRP samples (Table 3A).

TABLE 2.

1. Reparative tissues with bonding
   - 2 points: Bilaterally bonds with surrounding meniscus.
   - 1 point: Partially bonds with surrounding meniscus.
   - 0 points: No bond with surrounding meniscus.
2. Existence of fibrochondrocytes
   - 2 points: Fibrochondrocytes exist diffusely in the reparative tissues.
   - 1 point: Fibrochondrocytes are localized in the reparative tissues.
   - 0 points: No fibrochondrocytes in the reparative tissues.
3. Staining with Safranin-O
   - 2 points: Densely stained with safranin-O.
   - 1 point: Faintly stained with safranin-O.
   - 0 points: Not stained with safranin-O.

Effects of PRP on meniscal cell proliferation and sGAG synthesis. MTS assay was used as a measurement of cell viability. MTS assay revealed that PRP upregulated the viability of meniscal cells in a dose-dependent manner. PPP slightly activated meniscal cell viability, although the effect of PPP was limited, and downregulation of meniscal cell viability was observed when 30% PPP was added. The effect of PRP was significantly greater than that of PPP (Fig. 1). Comparable results for differences in proliferation behavior, expressed as the amount of newly synthesized DNA, are shown in Table 3B. BrdU assay revealed that there was more DNA synthesis in meniscal cells in the presence of PRP than in the presence of PPP or in the control (supplement-free medium). These results indicate that PRP promotes meniscal cell proliferation.

Quantification of the sGAG synthesized by meniscal cells in medium after 8 days of culture was determined to evaluate the cellular function using Alcian blue-binding assay. As shown in Table 3C, the density of sGAG in the mixed gathered mediums was significantly higher in the presence of PRP than in supplement-free medium (control) or PPP ($p < 0.01$). These results indicate that PRP promotes sGAG synthesis in meniscal cells.

Effects of PRP on gene expression of meniscal cell-related proteins. The results of meniscal cell-related messenger ribonucleic acid (mRNA) expressions after culture with 10% PRP, 10% PPP, and control medium are shown in Table 3D. All results are reported as relative mRNA expression in the control. First we examined the effect of PRP on the gene expression level of collagen 1. No significant change was found in the expression of collagen 1 mRNA in each sample. Next we examined the effect of PRP on the gene expression level of proteoglycans (PGs). Aggrecan mRNA expression fell approximately twice as much in the PRP samples as in the control samples ($p < 0.05$). There

Table 3. *In Vitro* Data

(a) ELISA

	PRP	*PPP*
PDGF-BB (ng/mL)	*3.23 ± 1.50	0.12 ± 0.06
TGF-β1 (ng/mL)	**78.41 ± 52.71	4.66 ± 3.67
VEGF (pg/mL)	**138.79 ± 53.79	19.44 ± 2.35

Values are expressed as the mean ± standard deviation.
*$p < 0.001$ compared with PPP group.
**$p < 0.005$ compared with PPP group.

(b) BrdU assay

	Control	*PRP*	*PPP*
absorbance (450–690 nm)	0.14 ± 0.01	*1.00 ± 0.02	0.30 ± 0.07

Values are expressed as the mean ± standard deviation.
*$p < 0.05$ compared with control and PPP groups.

(c) Alcian blue-binding assay

	Control	*PRP*	*PPP*
sGAG synthesis (μg/mL)	3.63 ± 0.50	*10.32 ± 0.96	8.11 ± 1.71

Values are expressed as the mean ± standard deviation.
*$p < 0.01$ compared with control and PPP groups.

(d) Real-time PCR (Relative mRNA expression in the control)

	PRP	*PPP*
Col 1	1.26 ± 0.90	1.38 ± 1.13
Aggrecan	+0.52 ± 0.22	1.28 ± 0.77
Biglycan	*2.10 ± 1.00	1.45 ± 0.88
Decorin	*4.71 ± 2.31	1.45 ± 0.49

Values are expressed as the mean ± standard deviation.
+Down regulation ($p < 0.05$) compared with control and PPP groups.
**Up regulation ($p < 0.05$) compared with control and PPP groups.

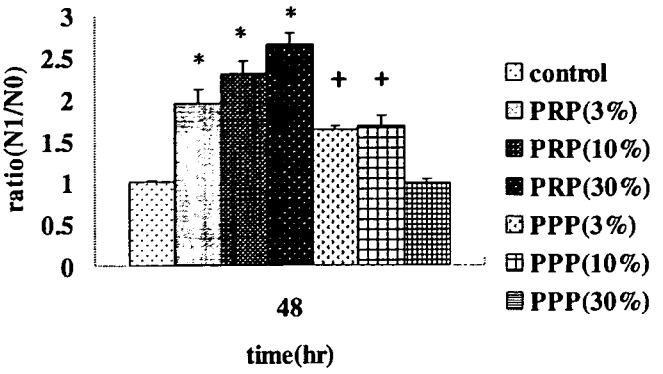

FIG. 1. 3-(4,5-dimethylthiazol-2yl)-5-(3-carboxymethoxyphenyl) -2-(4-sulfophenyl)-2H-tetrazolium inner salt assay measurement to evaluate cell viability. Platelet-rich plasma (PRP) upregulates the viability of meniscal cells in a dose-dependent manner ($*p < 0.05$). The effect of PRP is significant compared with the same dose of platelet-poor plasma ($^{+}p < 0.05$).

was no significant change in aggrecan mRNA expression between PPP and control. Measurements of mRNA expression of small PGs were also performed. Biglycan mRNA expression was more than twice as high in the PRP samples as in control samples ($p < 0.05$) and a fold increase in decorin mRNA expression was more than four times as high ($p < 0.05$). Furthermore, mRNA expression of both small PGs were upregulated significantly more in PRP samples than in samples ($p < 0.05$).

In vivo *study*

All the rabbits were moving freely in their cages by the second postoperative day. No evidence of postoperative infection at the wound site was observed, and all the wounds healed uneventfully. In the synovial tissue, slight hypertrophy was observed in the knees of some animals. No clear degeneration of articular cartilage of the femur or tibia was found.

Histological findings at 4 and 12 weeks are shown in Figures 2A–F and 3A–F. The results of semi-quantitative scoring are shown in Figure 4. Reparative tissue bonding scores over time in group A (treated with PRP) and group B (treated with PPP) are shown. In group C (treated with hydrogel only), the scores were almost the same each week. At every time point, the group A scores were higher than those in the other two groups, but these results were not statistically significant, except for the difference in results between groups A and B at 4 weeks.

The reparative tissues of groups B and C were mostly occupied with fibrous connective tissue and spindle-shaped fibroblast-like cells at every time point. At 8 weeks, some samples in group B contained a few oval-shaped cells, although the cells were localized in their sections, and the number had not increased much by 12 weeks. In group A, some oval-shaped cells could be found as early as 4 weeks.

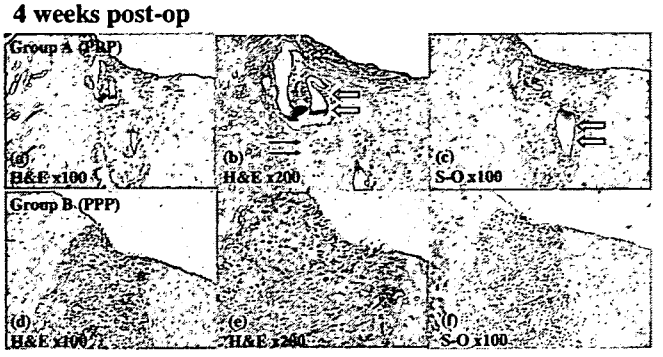

FIG. 2. Photomicrographs of the reparative tissues at 4 weeks. Sections of (**A–C**) are treated with platelet-rich plasma, Group A. Sections of (**D–F**) are treated with platelet-poor plasma, group B. **B** and **D** are the sections stained with hematoxylin and eosin (H–E) (magnification ×100), and **B** and **E** are the same staining with high magnification (×200). **C** and **F** are the sections stained with Safranin-O (S-O) (×100). In group A (**B**), the group A defects contained oval-shaped cells and relatively rich extracellular matrix components (black arrow), which were faintly stained with safranin-O. (**C**) Gelatin hydrogels remained in the defects at 4 weeks (open arrow). Group B defects are filled with Safranin-O negative fibrous tissue (**D–F**).

The scores of group A increased in a time-dependent manner, and at 12 weeks, many oval-shaped chondrocyte-like cells with unevenly spaced lacunae were diffusely present in the reparative tissues in almost all group A samples. The morphology resembled the inner zone of the meniscus. The group A score was statistically higher than the other 2 groups at 12 weeks.

The Safranin-O–positive ECM in the reparative tissues were examined and scored. In groups B and C, the reparative

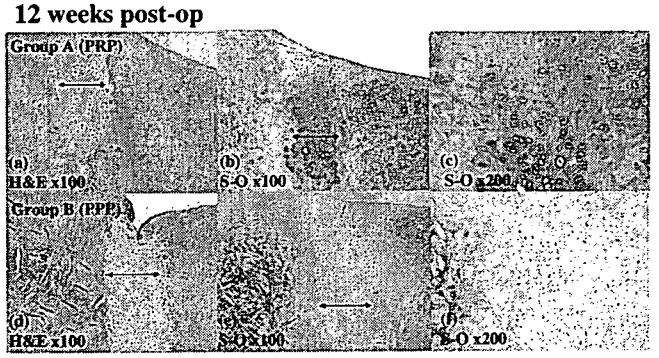

FIG. 3. Photomicrographs of the reparative tissues (arrow) at 12 weeks. Sections of **A–C** are group A and sections of **D–F** are group B. **A** and **D** are the sections stained with hematoxylin and eosin (H-E). (×100). **B** and **E** are the sections stained with Safranin-O (S-O) (×100), and **C** and **F** are the same staining with high magnification (×200). In group A, (**B, C**) the reparative tissues consist of Safranin-O–positive matrix with unevenly spaced lacunae. In contrast, group B defects are filled with Safranin-O negative fibrous tissue (**E, F**).

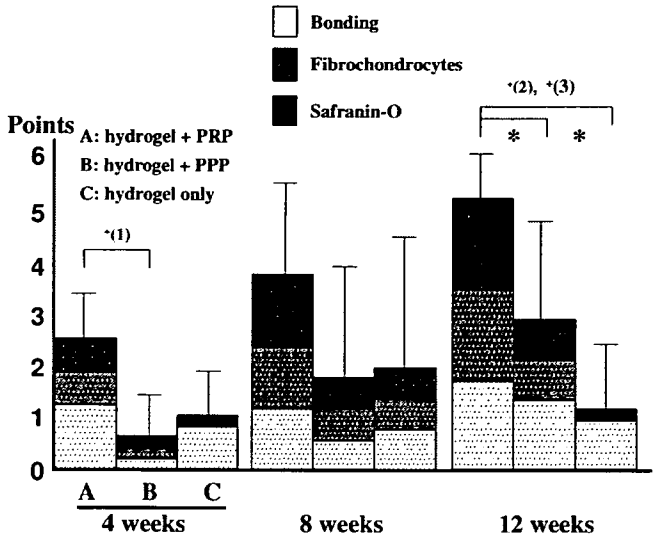

FIG. 4. The results of semi-quantitative scoring *in vivo*. Each average score is presented. Group A total score was significantly higher than that of the other 2 groups at 12 weeks ($*p < 0.05$). $^{+}(1)$ Reparative tissue bonding score in group A was significantly higher than in group B at 4 weeks. $^{+}(2)$ Scores showing the existence of fibrochondrocytes in group A were statistically higher than in the other 2 groups at 12 weeks. $^{+}(3)$ The scores of Safranin-O (S-O) staining in group A were significantly higher than in the other 2 groups at 12 weeks.

tissues looked fibrous with hematoxylin and eosin staining, and the tissues showed almost no staining with Safranin-O at any time point. In group A, although a relatively abundant ECM with oval-shaped cells existed at 4 weeks, the matrix was not stained with safranin-O. However, the group A score increased in a time-dependent manner, and at 12 weeks, the group A filled tissues were well stained with Safranin-O in almost all samples. The group A score was also statistically higher than the other 2 groups at 12 weeks.

There were some samples showing remnants of the hydrogel in every group at 4 weeks, although the remnants had disappeared by 8 weeks.

DISCUSSION

The menisci play important roles in knee function, including loading, shock absorption, proprioception, maintenance of joint stability, and lubrication.[1–8] Injury to the inner avascular part of the meniscus does not heal spontaneously; therefore, arthroscopic resection of the meniscus has been widely performed. However, repair of the inner avascular part of the meniscus is challenging for orthopedic surgeons.

In tissue-engineering approaches from cytokine therapy, several growth factors have been investigated and proven to be effective in meniscal tissue regeneration.[12–14,16] In the current study, we used PRP as an autologous growth factos, and the results showed the remarkable healing properties of PRP for the repair of the inner avascular part of meniscal injury *in vitro* and *in vivo*.

PRP was known as a concentrated suspension of growth factors, such as PDGF, TGF-β, VEGF, IGF-I, and endothelial cell growth factor.[20] These individual growth factors are well known to be effective for meniscal cells. For example, it has been demonstrated that the effect of TGF-β1 was dose-dependent, focusing on the PG synthesis of meniscal tissues,[15,16] and PDGF was considered to be one of most potent factors for mitogenic response in meniscal cells.[12,13,17] Because PRP was an autologous source, there was no risk of antibody formation or infection. Thus, platelets are a promising source of autologous growth factors, and if PRP growth factors could be effective for meniscal tissue, growth factor–promoted meniscal healing was anticipated.

In our study, PRP preparations concentrated over 1 million/μL platelets and therefore could be recognized as "therapeutic PRP."[20,30,31] Furthermore, the contained growth factors in our PRP preparations were also comparable with the PRP, prepared from commercial tube technique, further described as PRP1 (Curasan AG, Kleinostheim, Germany).[25–29] Thus, we consider our PRP preparations sufficient for investigating its effects on meniscal cells.

In the current *in vitro* study, we showed the effectiveness of PRP not only for its proliferating effect on meniscal cells, but also for synthesizing GAG. GAG was important for the meniscus, as well as hyaline cartilage, and the phenotype of the inner avascular region of the meniscus was fibrocartilage-like, and it was known that the cells isolated from this region produce more GAGs in culture than cells from the peripheral region.[15,46] In Table 3A, PPP also stimulated GAG synthesis more than control on meniscal cells; we supposed that it depended on a few platelets contained in PPP.

The results of real-time PCR study to assess the PRP were interesting. Aggrecan was a main, large aggregating PG in hyaline cartilage. Aggrecan in meniscus showed an organized, spatial network, in contrast to its diffuse distribution in articular cartilage, and contributed to the pool in the synovial fluid.[47] When hyaline cartilage regeneration was considered, the downregulation of aggrecan mRNA expression would not be desired. In fact, some reports have revealed that platelet supernatant activated chondrocyte proliferation but induced a dedifferentiation of chondrocytes toward fibroblast-like phenotypes in monolayer and 3-dimensional alginate cultures.[48,49] However, when considering meniscal tissue regeneration, it remained to be seen whether these changes in mRNA expression would lead to the fibrocartilage desired, for the following reasons. The native meniscus itself actually had a low PG content,[14] and the ratio of PG was different from hyaline cartilage, which was largely composed of aggrecan. Small PG (decorin and biglycan) and aggrecan have previously been

extracted in a weight ratio of approximately 1:1 in the adult human meniscus; thus, the amount of small PG was high.[50] Roughley *et al.* stated that the presence of aggrecan and small PG might be a common feature of the need to resist compressive and tensile forces in the meniscus.[50] As we saw, real-time PCR study in monolayer meniscal cells cultured with PRP revealed upregulations of small PG mRNA expressions. This result indicates that PRP induces the meniscal cells toward fibrocartilage-like phenotypes, suggesting that PRP is a more attractive and favorable source for fibrocartilage than for hyaline cartilage.

In general, the lives of many growth factors are too short to sustain biological activity *in vivo*. PRP growth factors were initiated and secreted from platelets through blood clotting, and more than 95% of the presynthesized growth factors were secreted within 1 h.[20] It was therefore likely that free PRP diffused into the knee joint rapidly and would result in no exertion of growth factor activity. Therefore, a single local application of PRP would be unlikely to achieve successful tissue regeneration.

One method that was needed for *in vivo* application was controlled release. Tabata *et al.* reported a controlled-release system composed of acidic gelatin with an isoelectric point of 5.0, which forms a poly-ionic complex with growth factors, and they demonstrated that the controlled release of growth factors from the hydrogel of acidic gelatin promoted bone regeneration in rabbit and monkey skull defects.[39,40,42] The growth factors were immobilized in the hydrogel through a physicochemical interaction with gelatin molecules, and the immobilized growth factors were released from the hydrogel as a result of hydrogel degradation.[32] As a source of sustained delivery of PRP growth factors, we also used acidic gelatin hydrogels.

In the current *in vivo* study, almost all the defects in group A (hydrogels with PRP) were healed with ECM-rich fibrocartilages at 12 weeks. We considered the healing process to occur as in Figure 5. First, it was the healing process called "intrinsic repair" (meniscal fibrochondrocytes activation).[51] In our *in vivo* study, round cells and rich ECM formations were seen as early as 4 weeks, and progress toward fibrocartilage occurred gradually. Furthermore, we have shown the effectiveness of PRP with rabbit meniscal cells *in vitro*. It was therefore possible that the surrounding meniscal cells played some part in the process of meniscal repair.

In addition to intrinsic repair, extrinsic repair (neovascularization and formation of granulation tissue) has also been reported to be important in meniscal regeneration.[51,52] In the early stages of our study, some samples in the histological analysis showed pannus-like tissues invading the surface of the meniscus through the synovium to the meniscal defect. It was possible that synovial cells (containing synovium-derived MSCs[53]) also played a part in the process of meniscal repair.

In some samples at 4 weeks, like Figure 2A–C, there were still some remnants of hydrogel in the meniscal defect. The

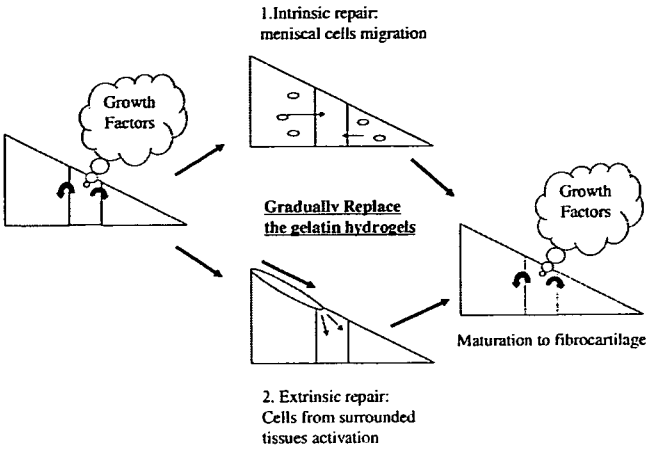

FIG. 5. The process of meniscal repair with hydrogels incorporating platelet-rich protein (PRP). When hydrogels incorporating PRP fill the defect, the growth factors are released as the hydrogels biodegrade. We believe that the growth factors activated 2 processes as follows. 1. Fibrochondrocytes derived from the surrounding meniscus were activated and migrated into the defect (intrinsic repair) (middle upper schema). 2. Synovium-derived MSCs or other multi-potent cells were activated and migrated into the defect through the surface of the surrounding meniscus (extrinsic repair) (middle lower schema) together. These cells migrated into the defects and gradually replaced the gelatin hydrogels. PRP growth factors further stimulated these migrated cells, which eventually directly matured to fibrocartilage (right side schema).

acidic hydrogels were designed to biodegrade some individual growth factors in an average of approximately 2 weeks under the *in vivo* conditions,[32,42] although the detailed degradation characteristics were unclear when various growth factors, like PRP, were added to the meniscal defect. We hypothesized that *in vivo* conditions might be different for different locations and different degradation characteristics could occur when rich growth factors, like PRP, were applied. In our histological findings, there were no remnants of the hydrogel after 8 weeks, so we were convinced that the acidic hydrogels were biodegraded and could control release of PRP growth factors for about 4 weeks in our *in vivo* study.

In conclusion, it appeared that PRP enhanced the healing properties of the inner avascular part of meniscal cells. It is likely that growth factors contained in PRP enhanced the biological activities of the meniscal cells for meniscal tissue regeneration. In the current *in vivo* application for rabbit meniscal defects, we found that the reparative fibrocartilaginous tissues closely resembled the inner portions of the normal meniscus, whereas borders between normal and reparative tissues existed histologically. Further investigation was needed to evaluate the biomechanical properties of this reparative tissue, although we believed that PRP was an effective biomaterial for meniscal tissue regeneration.

REFERENCES

1. Fukubayashi, T., and Kurosawa H. The contact area and pressure distribution pattern of the knee. A study of normal and osteoarthrotic knee joints. Acta Orthop Scand **51,** 871, 1980.
2. Krause, W.R., Pope, M.H., Johnson, R.J., and Wilder, D.G. Mechanical changes in the knee after meniscectomy. J Bone Joint Surg Am **58,** 599, 1976.
3. Eggli, S., Wegmuller, H., Kosina, J., Huckell, C., and Jakob, R.P. Long-term results of arthroscopic meniscal repair. An analysis of isolated tears. Am J Sports Med **23,** 715, 1995.
4. Johnson, R.J., Kettelkamp, D.B., Clark, W., and Leaverton, P. Factors effecting late results after meniscectomy. J Bone Joint Surg Am **56,** 719, 1974.
5. Markolf, K.L., Bargar, W.L., Shoemaker, S.C., and Amstutz, H.C. The role of joint load in knee stability. J Bone Joint Surg Am **63,** 570, 1981.
6. Dandy, D.J., and Jackson, R.W. Meniscectomy and chondromalacia of the femoral condyle. J Bone Joint Surg Am **57,** 1116, 1975.
7. Radin, E.L., de Lamotte, F., and Maquet, P. Role of the menisci in the distribution of stress in the knee. Clin Orthop Relat Res **185,** 290, 1984.
8. Kurosawa, H., Fukubayashi, T., and Nakajima, H. Load-bearing mode of the knee joint: physical behavior of the knee joint with or without menisci. Clin Orthop Relat Res **149,** 283, 1980.
9. Seedhom, B.B., and Hargreaves, D.J. Transmission of the load in the knee joint with special references to the role of the menisci. II. Experimental results, discussion and conclusions. Eng Med **8,** 220, 1979.
10. Ochi, M., Uchio, Y., Okuda, K., Shu, N., Yamaguchi, H., and Sakai, Y. Expression of cytokines after meniscal rasping to promote meniscal healing. Arthroscopy **17,** 724, 2001.
11. McAndrews, P.T., and Arnoczky, S.P. Meniscal repair enhancement techniques. Clin Sports Med **15,** 499, 1996.
12. Bhargava, M.M., Attia, E.T., Murrell, G.A., Dolan, M.M., Warren, R.F., and Hannafin J.A. The effect of cytokines on the proliferation and migration of bovine meniscal cells. Am J Sports Med **27,** 636, 1999.
13. Lietman, S.A., Hobbs, W., Inoue, N., and Reddi, A.H. Effects of selected growth factors on porcine meniscus in chemically defined medium. Orthopedics **26,** 799, 2003.
14. Buma, P., Ramrattan, N.N., van Tienen, T.G., and Veth, R.P. Tissue engineering of the meniscus. Biomaterials **25,** 1523, 2004.
15. Collier, S., and Ghosh, P. Effects of transforming growth factor beta on proteoglycan synthesis by cell and explant cultures derived from the knee joint meniscus. Osteoarthritis Cartilage **3,** 127, 1995.
16. Imler, S.M., Doshi, A.N., and Levenston, M.E. Combined effects of growth factors and static mechanical compression on meniscus explant biosynthesis. Osteoarthritis Cartilage **12,** 736, 2004.
17. Webber, R.J., Harris, M.G., and Hough, A.J., Jr. Cell culture of rabbit meniscal fibrochondrocytes: proliferative and synthetic response to growth factors and ascorbate. J Orthop Res **3,** 36, 1985.
18. Slater, M., Patava, J., Kingham, K., and Mason, R.S. Involvement of platelets in stimulating osteogenic activity. J Orthop Res **13,** 655, 1995.
19. Sammartino, G., Tia, M., Marenzi, G., di Lauro, A.E., D'Agostino, E., and Claudio, P.P. Use of autologous platelet-rich plasma (PRP) in periodontal defect treatment after extraction of impacted mandibular third molars. J Oral Maxillofac Surg **63,** 766, 2005.
20. Marx, R.E. Platelet-rich plasma: evidence to support its use. J Oral Maxillofac Surg **62,** 489, 2004.
21. Fennis, J.P., Stoelinga, P.J., Merkx, M.A., and Jansen, J.A. Reconstruction of the mandible with a poly(D,L-lactide) scaffold, autogenous corticocancellous bone graft, and autogenous platelet-rich plasma: an animal experiment. Tissue Eng **11,** 1045, 2005.
22. Yamada, Y., Ueda, M., Naiki, T., Takahashi, M., Hata, K., and Nagasaka, T. Autogenous injectable bone for regeneration with mesenchymal stem cells and platelet-rich plasma: tissue-engineered bone regeneration. Tissue Eng **10,** 955, 2004.
23. Nikolidakis, D., van den Dolder, J., Wolke, J.G., Stoelinga, P.J., and Jansen, J.A. The effect of platelet-rich plasma on the bone healing around calcium phosphate-coated and non-coated oral implants in trabecular bone. Tissue Eng **12,** 2555, 2006.
24. Dolder, J.V., Mooren, R., Vloon, A.P., Stoelinga, P.J., and Jansen, J.A. Platelet-rich plasma: quantification of growth factor levels and the effect on growth and differentiation of rat bone marrow cells. Tissue Eng 2006 Oct 1; [Epub ahead of print].
25. Wiltfang, J., Kloss, F.R., Kessler, P., Nkenke, E., Schultze-Mosgau, S., Zimmermann, R., and Schlegel, K.A. Effects of platelet-rich plasma on bone healing in combination with autogenous bone and bone substitutes in critical-size defects. An animal experiment. Clin Oral Implants Res **15,** 187, 2004.
26. Schlegel, K.A., Donath, K., Rupprecht, S., Falk, S., Zimmermann, R., Felszeghy, E., and Wiltfang, J. De novo bone formation using bovine collagen and platelet-rich plasma. Biomaterials **25,** 5387, 2004.
27. Thorwarth, M., Wehrhan, F., Schultze-Mosgau, S., Wiltfang, J., and Schlegel, K.A. PRP modulates expression of bone matrix proteins *in vivo* without long-term effects on bone formation. Bone **38,** 30, 2006.
28. Thorwarth, M., Rupprecht, S., Falk, S., Felszeghy, E., Wiltfang, J., and Schlegel, K.A. Expression of bone matrix proteins during de novo bone formation using a bovine collagen and platelet-rich plasma (PRP)—an immunohistochemical analysis. Biomaterials **26,** 2575, 2005.
29. Tozum, T.F., and Demiralp, B. Platelet-rich plasma: a promising innovation in dentistry. J Can Dent Assoc **69,** 664, 2003.
30. Marx, R.E. Platelet-rich plasma (PRP): what is PRP and what is not PRP? Implant Dent **10,** 225, 2001.
31. Hokugo, A., Ozeki, M., Kawakami, O., Sugimoto, K., Mushimoto, K., Morita, S., and Tabata Y. Augmented bone regeneration activity of platelet-rich plasma by biodegradable gelatin hydrogel. Tissue Eng **11,** 1224, 2005.
32. Yamamoto, M., Ikada, Y., and Tabata, Y. Controlled release of growth factors based on biodegradation of gelatin hydrogel. J Biomater Sci Polym Ed **12,** 77, 2001.
33. Kawamoto, T., Akisue, T., Marui, T., Nakatani, T., Hitora, T., Fujita, I., and Kurosaka, M. Inhibitory effect of STI571 on cell proliferation of human malignant fibrous histiocytoma cell lines. Anticancer Res **24,** 2675, 2004.

34. Tsutsumi, K., Yasuda, M., and Nishioka, T. X-ray irradiation altered chemosensitivity of a p53-null non-small cell lung cancer cell line. Cell Struct Funct **31,** 47, 2006.
35. Maghni, K., Nicolescu, O.M., and Martin, J.G. Suitability of cell metabolic colorimetric assays for assessment of CD4 + T cell proliferation: comparison to 5-bromo-2-deoxyuridine (BrdU) ELISA. J Immunol Methods **223,** 185, 1999.
36. Cui, Y.L., Qi, A.D., Liu, W.G., Wang, X.H., Wang, H., Ma, D.M., and Yao, K.D. Biomimetic surface modification of poly(L-lactic acid) with chitosan and its effects on articular chondrocytes *in vitro*. Biomaterials **24,** 3859, 2003.
37. Bjornsson, S. Simultaneous preparation and quantitation of proteoglycans by precipitation with Alcian blue. Anal Biochem **210,** 282, 1993.
38. Sobajima, S., Shimer, A.L., Chadderdon, R.C., Kompel, J.F., Kim, J.S., Gilbertson, L.G., and Kang, J.D. Quantitative analysis of gene expression in a rabbit model of intervertebral disc degeneration by real-time polymerase chain reaction. Spine J **5,** 14, 2005.
39. Tabata, Y., Yamada, K., Hong, L., Miyamoto, S., Hashimoto, N., and Ikada, Y. Skull bone regeneration in primates in response to basic fibroblast growth factor. J Neurosurg **91,** 851, 1999.
40. Tabata, Y., and Ikada, Y. Vascularization effect of basic fibroblast growth factor released from gelatin hydrogels with different biodegradabilities. Biomaterials **20,** 2169, 1999.
41. Ozeki, M., and Tabata, Y. Promoted growth of murine hair follicles through controlled release of basic fibroblast growth factor. Tissue Eng **8,** 359, 2002.
42. Yamamoto, M., Tabata, Y., Hong, L., Miyamoto, S., Hashimoto, N., and Ikada, Y. Bone regeneration by transforming growth factor beta1 released from a biodegradable hydrogel. J Control Release **64,** 133, 2000.
43. Makino, T., Fujioka, H., Kurosaka, M., Matsui, N., Yoshihara, H., Tsunoda, M., and Mizuno, K. Histologic analysis of the implanted cartilage in an exact-fit osteochondral transplantation model. Arthroscopy **17,** 747, 2001.
44. Makino, T., Fujioka, H., Terukina, M., Yoshiya, S., Matsui, N., and Kurosaka, M. The effect of graft sizing on osteochondral transplantation. Arthroscopy **20,** 837, 2004.
45. Kobayashi, K., Fujimoto, E., Deie, M., Sumen, Y., Ikuta, Y., and Ochi, M. Regional differences in the healing potential of the meniscus-an organ culture model to eliminate the influence of microvasculature and the synovium. Knee **11,** 271, 2004.
46. Tanaka, T., Fujii, K., and Kumagae, Y. Comparison of biochemical characteristics of cultured fibrochondrocytes isolated from the inner and outer regions of human meniscus. Knee Surg Sports Traumatol Arthrosc **7,** 75, 1999.
47. Valiyaveettil, M., Mort, J.S., and McDevitt, C.A. The concentration, gene expression, and spatial distribution of aggrecan in canine articular cartilage, meniscus, and anterior and posterior cruciate ligaments: a new molecular distinction between hyaline cartilage and fibrocartilage in the knee joint. Connect Tissue Res **46,** 83, 2005.
48. Yang, S.Y., Ahn, S.T., Rhie, J.W., Lee, K.Y., Choi, J.H., Lee, B.J., and Oh, G.T. Platelet supernatant promotes proliferation of auricular chondrocytes and formation of chondrocyte mass. Ann Plast Surg **44,** 405, 2000.
49. Gaissmaier, C., Fritz, J., Krackhardt, T., Flesch, I., Aicher, W.K., and Ashammakhi, N. Effect of human platelet supernatant on proliferation and matrix synthesis of human articular chondrocytes in monolayer and three-dimensional alginate cultures. Biomaterials **26,** 1953, 2005.
50. Roughley, P.J., and White, R.J. The dermatan sulfate proteoglycans of the adult human meniscus. J Orthop Res **10,** 631, 1992.
51. Arnoczky, S.P., Warren, R.F., and Spivak, J.M. Meniscal repair using an exogenous fibrin clot. An experimental study in dogs. J Bone Joint Surg Am **70,** 1209, 1988.
52. Hashimoto, J., Kurosaka, M., Yoshiya, S., and Hirohata, K. Meniscal repair using fibrin sealant and endothelial cell growth factor. An experimental study in dogs. Am J Sports Med **20,** 537, 1992.
53. Sakaguchi, Y., Sekiya, I., Yagishita, K., and Muneta, T. Comparison of human stem cells derived from various mesenchymal tissues: superiority of synovium as a cell source. Arthritis Rheum **52,** 2521, 2005.

Address reprint requests to:
Ryosuke Kuroda, M.D.
Department of Orthopedic Surgery
Kobe University Graduate School of Medicine
7-5-1 Kusunoki-cho, Chuo-ku,
Kobe 650-0017
Japan

E-mail: kurodar@med.kobe-u.ac.jp

Controlled release of basic fibroblast growth factor promotes healing of the pancreaticojejunal anastomosis: A novel approach toward zero pancreatic fistula

Takayuki Aimoto, MD,[a] **Eiji Uchida, MD,**[a] **Akira Matsushita, MD,**[a] **Yasuhiko Tabata, PhD, D Med Sci, D Pharm,**[b] **Teruo Takano, MD,**[c] **Masaaki Miyamoto, MD,**[c] *and* **Takashi Tajiri, MD,**[a] *Tokyo and Kyoto, Japan*

Background. *Several reconstructive surgical techniques have been proposed for restoring pancreaticojejunal continuity. Little has been done, however, to evaluate the efficacy of tissue engineering on anastomotic healing. We examined the effects of basic fibroblast growth factor (bFGF) incorporated in gelatin hydrogel (GH) microspheres on the anastomotic healing of pancreaticojejunostomy.*
Methods. *As a preliminary experiment, 20 female Wistar rats received a jejunal subserosal injection of 1 μg of bFGF-GH (n = 10), 1 μg of Free-bFGF (n = 5), or gelatin alone (n = 5) to study the effects of bFGF on the histology of normal jejunum on day 7 after the injection. Next, 12 beagle dogs received a jejunal subserosal injection of 100-μg bFGF-GH (n = 7) or gelatin alone (n = 5) at the anastomotic site of pancreaticojejunostomy. Four types of assessment were performed to compare the 2 groups: pancreatography, breaking strength test, pathologic examination, and calculation of the microvessel density (MVD).*
Results. *The bFGF-GH injection led to markedly increased levels of collagen and fibroblastic cellularity in the subserosal layer of the Wistar rats. In contrast, the rats treated by gelatin alone exhibited no such effects. No anastomotic failures were observed in the dogs treated by bFGF-GH. Histologic observations of this group revealed abundant granulation tissues. Treatment with bFGF-GH significantly increased the breaking strength and MVD over the levels measured in the control group (P < .01).*
Conclusions. *bFGF-GH accelerates healing of pancreaticojejunal anastomosis during the early postoperative period. Basic FGF-GH may show promise as a new technique for preventing anastomotic failure of pancreaticojejunostomy. (Surgery 2007;142:734-40.)*

From the Department of Surgery, Nippon Medical School, Tokyo, Japan[a]*; Department of Biomaterials, Institute for Frontier Medical Sciences, Kyoto University, Kyoto, Japan*[b]*; and the Department of Internal Medicine, Nippon Medical School, Tokyo, Japan*[c]

POSTOPERATIVE MORBIDITY AFTER PANCREATICODUODENECTOMY (PD) remains high.[1,2] Pancreatic fistula (PF) is the most important morbidity and may cause secondary complications.[1] Recent studies have proposed modified anastomotic techniques and novel pharmacologic approaches to prevent PF.[3-6] The modified anastomotic techniques have had some success in reducing PF, but none have eliminated it completely.

The essential role of growth factors in the formation of granulation tissue in wound healing has been established.[7,8] Several studies applying basic fibroblast growth factor (bFGF) to wound healing suggest that bFGF serves as a key factor to accelerate wound healing by promoting fibroblast proliferation and neovascularization.[9-12] When bFGF is used in its free form, the very short duration of its activation in vivo may prevent it from conferring biologic effects.

Tissue engineering is a new biomedical technology designed to create an environment for tissue regeneration.[13,14] Growth factors released from gela-

Supported by a grant-in-aid from the Japan Society for the Study of Surgical Techniques. The recombinant bFGF was provided by Kaken Pharmaceutical Co., Ltd., Tokyo, Japan, and the J-VAC drainage system was supplied by Johnson & Johnson Co., Tokyo, Japan.

Accepted for publication March 31, 2007.

Reprint requests: Takayuki Aimoto, MD, Department of Surgery, Nippon Medical School, 1-1-5 Sendagi, Bunkyo-ku, Tokyo 113-8603, Japan. E-mail: aimoto@nms.ac.jp.

0039-6060/$ - see front matter

doi:10.1016/j.surg.2007.03.016

tin controlled-release systems retain their biologic activity.[13,14] Tabata et al[14] developed a technique to incorporate bFGF in gelatin hydrogel microspheres. The result, the bFGF-incorporated gelatin hydrogel microsphere (bFGF-GH), has been applied as a useful system for delivery and controlled release in several studies on organ reconstruction.[15,16]

Little has been done to evaluate the efficacy of bFGF-GH on anastomotic healing. As a novel approach toward zero PF, our group examined the efficacy of bFGF-GH on the anastomotic healing of pancreaticojejunostomy (PJ).

MATERIALS AND METHODS

Preparation of the bFGF-incorporated gelatin hydrogel microspheres. Gelatin with an isoelectric point (IPEs) of 5.0 was prepared through an alkaline process of bovine bone collagen and named "acidic gelatin" (Nitta Gelatin Co., Osaka, Japan). Gelatin hydrogels were prepared through glutaraldehyde crosslinking of the acidic gelatin in an aqueous solution.[17] Basic FGF-GH was obtained by dropping 200 μL of distilled water with bFGF (100 μg) onto 20 mg of gelatin hydrogels and left overnight at 4°C.

Preparation of the animals. These studies were performed in accordance with the guidelines for Animal Experiments of the Nippon Medical School and Nippon Veterinary and Animal Science University, all of which conformed with the Legal Guidance on the Care and Use of Laboratory Animals in Japan. Fifteen-week-old female Wistar rats weighing 230 to 250 g were obtained from Shizuoka Laboratory Animal Center (Shizuoka, Japan) (n = 20) and fed standard rat food and tap water ad libitum for 7 days before the injections to study the effects of bFGF on the histology of normal jejunum. Twelve beagle dogs weighing 10-15 kg were obtained from the Institute for Animal Reproduction (Ibaragi, Japan) and housed in an accredited facility on a 12 h:12 h, light:dark cycle with access to food and water ad libitum for use as the animal PJ model.

Experimental design and operative procedure. *Implantation of bFGF-GH into the subserosal layer of the intestine in the rat model:* This study was designed to examine the effect of bFGF-GH on the subserosal injection of the intestine. The rats were divided into 3 groups: 1) the bFGF-GH group (n = 10) injected with 1 μg of bFGF-GH, 2) the Free-bFGF group (n = 5) injected with 1 μg of bFGF, and 3) the control group (n = 5) injected with gelatin hydrogel alone. A median laparotomy was performed under ether anesthesia. The jejunum was pulled out from the abdominal wound from a point 10 cm distal to the pyloric ring and injected a 1 μg dose of bFGF-GH with 0.1-mL saline using a 1-mL syringe subserosally. All animals were killed under deep ether anesthesia on day 7 after the procedure. The injected-intestine was resected for examination by macroscopic observation and hematoxylin-eosin (HE) and Masson's trichrome (MT) staining.

Implantation of the bFGF-GH into the anastomotic site of the pancreaticojejunostomy in the beagle dog model: All animals were fasted for 24 h preoperatively. The procedure began with intubation via the trachea under general anesthesia commenced by a subcutaneous injection of medetomidine hydrochloride (20 μ/kg) (Meiji, Tokyo, Japan), meloxicam (Boehringer Ingelheim, Burlington, Canada), and midazolam (0.3 mg/kg) (Astellas, Tokyo, Japan). The anesthesia was maintained during the procedure by mechanical ventilation with a mixture of isoflurane and oxygen, together with epidural anesthesia (10 μg/kg of 0.5% bupivacaine hydrochloride). Intravenous lactated Ringer's solution was also administered during the procedure. Once the midline incision was cut, the pancreas was divided into 2 parts at the mid-body, the right lobe was left in situ with its duct ligated distally, and a continuous suture was sewn for hemostasis. A Roux-en-Y side-to-end PJ to the left lobe was constructed as a 1-layer anastomosis with a stent (sheath of a 24G polyethylene needle). The pancreatic parenchyma was sutured to the jejunal seromuscular layer by placing 4 stitches with an interrupted suture (6-0 nonabsorbable monofilament suture).

The dogs in this study were divided into 2 groups: 1) a bFGF-GH group (n = 7) receiving a jejunal subserosal injection of bFGF-GH (100 μg) at the anastomotic site and 2) the control group (n = 5) receiving gelatin hydrogel alone. The dogs were killed on postoperative day 7 and underwent autopsy. The anastomoses were resected for macroscopic observation, histologic evaluation (HE and MT staining), pancreatography, the breaking strength test, and estimation of microvessel density.

The pancreatography was performed using a stent tube to confirm the patency of the pancreatic duct and incidence of anastomotic failure.

Breaking strength test. Breaking strength was measured by a spring balance. The tissues of anastomotic regions were cut into 5 × 5-mm squares and secured at 2 ends by binder clips. A force was applied across the anastomotic site at a constant speed (1 cm/s). Breaking strength was expressed as the point of maximal stress ($g/25\ mm^2$) before separation of the anastomosis.

Microscopic examination. Sections of the treated-intestines and anastomotic regions (4 μm in thickness) were fixed in 10% formalin, embedded in paraffin wax, and examined by HE and MT stain-

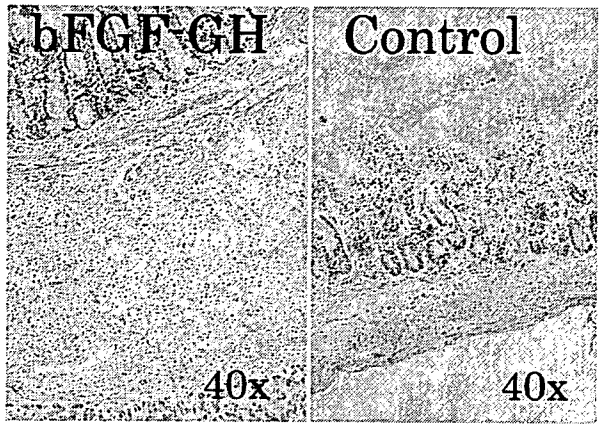

Fig 1. Microscopic appearance of a bFGF-GH-treated intestine and GH-treated intestine (control), HE, 40×. The fibroblast proliferation and collagen content were higher in the bFGF-GH group than in the control group.

ing. The following scoring index was used to evaluate the cellular composition (inflammatory cells and fibroblasts) and the collagen content, based on a modified 0-to-4 Ehrlich and Hunt numerical scale: 0 = no evidence, 1 = occasional evidence, 2 = light scattering, 3 = abundant evidence, and 4 = confluent cells or vessels.[18]

Immunohistochemistry: Microvessel detection and counting. The sections were stained for factor VIII–related antigen by the avidin–biotin–peroxidase complex (ABC)–immunoperoxidase method previously described.[19] In brief, the sections were incubated in a rabbit polyclonal anti-factor-VIII–related antigen (Dako Japan Co, Kyoto, Japan) at a 1:200 dilution at 4°C in a humid chamber. Peroxidase activity was visualized with diaminobenzidine tetrahydroxychloride solution (Nichirei Co., Tokyo, Japan) as substrate. The sections were counterstained lightly with Mayer's hematoxylin.

The slide was scanned systemically at ×40 magnification to identify the 3 areas with the greatest density of microvessels, so-called hot spots. The microvessel density (MVD) (/mm^2) was calculated by counting the microvessels in a single 200× field (0.78 mm^2 per field) in each hot spot.

The pathological examiners for the macroscopic and microscopic evaluation were blinded to the treatment in this study.

Statistical analysis. All data are given as mean ± standard deviation (SD). Statistical significance was tested using analysis of Mann-Whitney *U* test for unpaired or paired comparisons between groups. Statistical significance was accepted at $P < .05$.

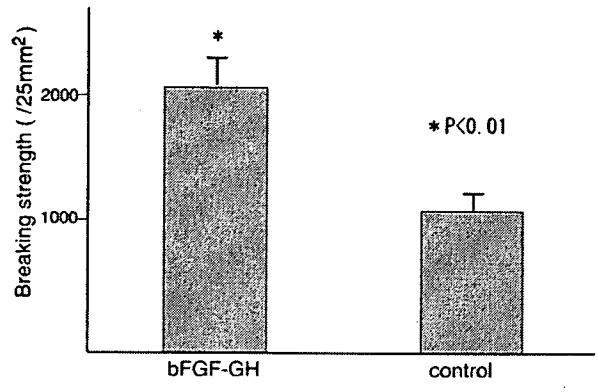

Fig 2. Results of the breaking strength test for the control group and the bFGF-GH group. The breaking strength was significantly higher in the bFGF-GH group than in the control group ($P < .01$).

RESULTS

Effects of the subserosal injection of bFGF-GH in the rat model. We evaluated the effect of bFGF-GH on subserosal tissue by injecting bFGF-GH into the subserosal layer of rat intestine.

Intestinal adhesion to the liver and marked wall thickness at the injection site were observed in the bFGF-GH group. In contrast, no remarkable changes were found in the control and free-bFGF groups.

Histologic examination revealed an increase in the thickness of the subserosal layer at the injection site of the bFGF-GH group versus normal intestine. The fibroblast proliferation and collagen content were higher in the bFGF-GH group than in the free-bFGF group (Fig 1).

Effects of bFGF-GH in the dog model of pancreaticojejunostomy. We evaluated the effect of bFGF-GH on PJ in an experimental model of PJ in dogs.

Macroscopic findings: All animals in this study survived the surgical procedures, and no anastomotic failure was observed in the bFGF-GH (0%) group. Anastomotic leakage was detected in 1 animal (20%) of the control group. The macroscopic appearance of the cross section at the anastomotic site in the bFGF-GH group was similar to that in the control group.

Pancreatography: The pancreatic duct was patent without stricture in all animals of all groups. Leakage was only found in 1 animal of the control group.

Breaking strength test: The breaking strength test was performed to evaluate the anastomotic strength. The breaking strength was significantly higher in the bFGF-GH group than in the control group (2074.7 ±

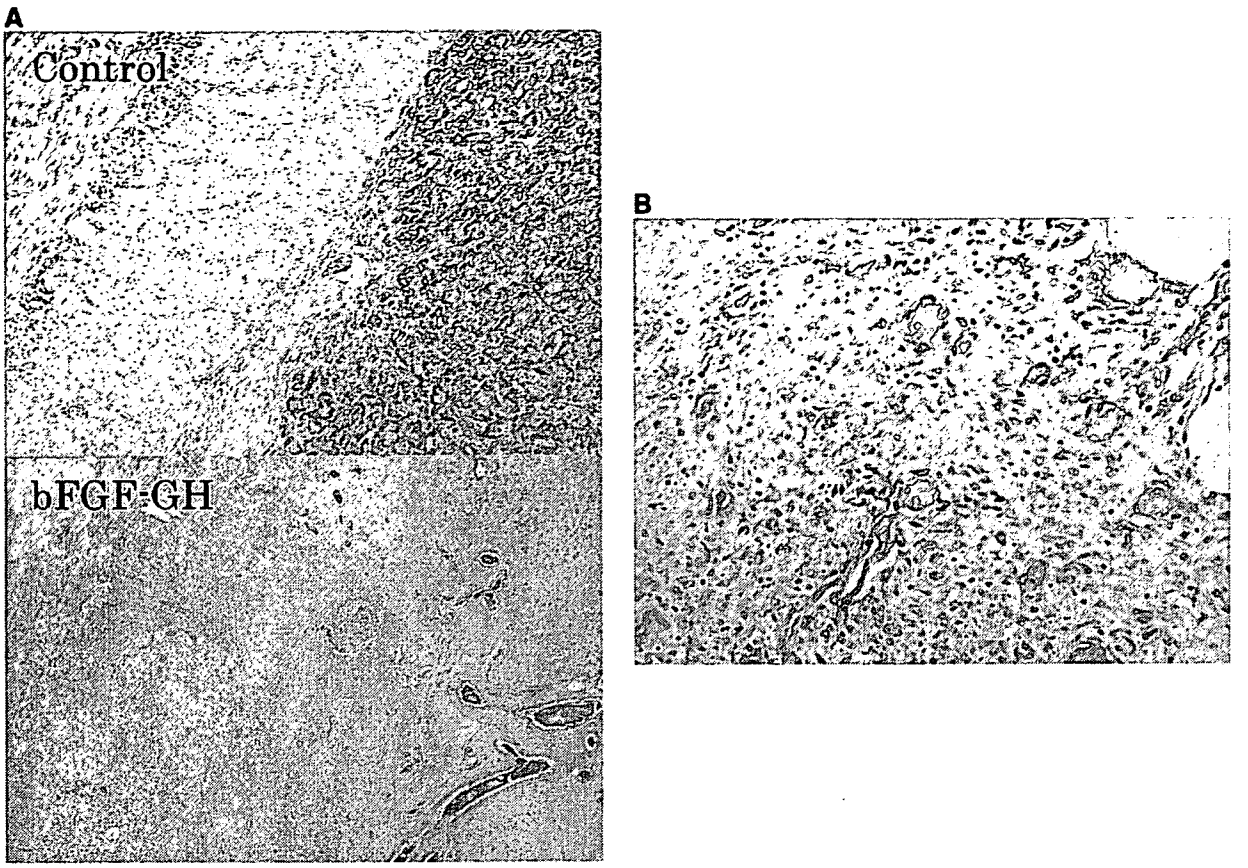

Fig 3. A, PJ anastomosis in the bFGF-GH group and the control group, HE, 40×. The border zone of the anastomotic site in the control group consisted of only small amounts of granulation tissue compared with the bFGF-GH group. **B,** The anastomotic site of the bFGH-GH group exhibited abundant granulation tissue composed of dense collagen and a proliferation of fibroblasts and new capillaries, HE, 100×.

114.7 g/25 mm^2 versus 1100 ± 51 g/25 mm^2, $P <$ .01) (Fig 2).

Microscopic examination: The border zone of the anastomotic site in the control group consisted of only small amounts of granulation tissue. In contrast, the anastomotic site of the bFGH-GH group exhibited abundant granulation tissue composed of dense collagen and a proliferation of fibroblasts and new capillaries (Fig 3, *A and B*). Indices for inflammatory cells, fibroblast proliferation, and collagen content were significantly higher in the bFGF-GH group than in the control group ($P <$ .01) (Fig 4).

Microvessel density (MVD): Hot spots were identified in the border zone of anastomotic sites in both groups. The MVD was significantly higher in the bFGF-GH group than in the control group (55.6 ± 8.8/mm^2 vs 11 ± 3.2/mm^2, $P <$ .01) (Fig 5).

DISCUSSION

Pancreatic fistula (PF) remains the most important cause of morbidity after PD and still contributes to mortality.[1,2] The current focus in pancreatic surgery is to reduce the incidence of PF by constructing a safe anastomosis.[1,2] Various techniques for managing the pancreatic remnant have been studied in relation to anastomotic leakage.[1,2] Prospective randomized controlled studies show no difference between the rates of PF after PJ and pancreaticogastrostomy (PG), the 2 most commonly applied methods for reconstruction after pancreatectomy.[3,4] Recent randomized controlled studies comparing PJ invagination anastomosis to duct-to-mucosa anastomosis show very similar rates of complication.[1,2] Specialized centers now achieve a PF of less than 5% to 10% irrespective of the anastomotic method.[1] A 0 PF has not yet been achieved.

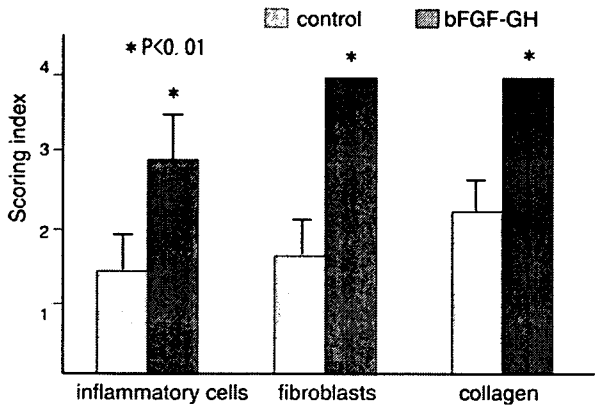

Fig 4. The scoring indices for cellularity and collagen content. All scoring indices were significantly higher in the bFGF-GH group than in the control group ($P < .01$).

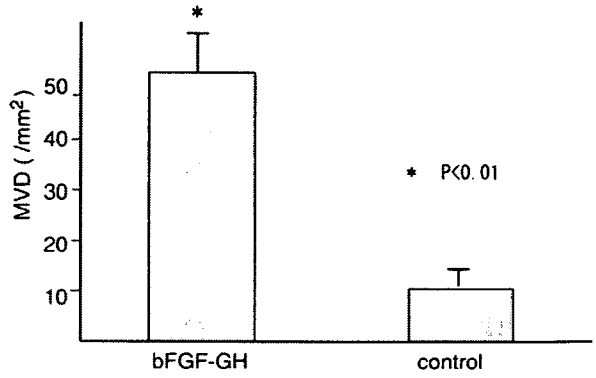

Fig 5. The MVD for both groups. The MVD was significantly higher in the bFGF-GH than in the control group ($P < .01$).

Several investigators have studied risk factors for PF through multivariate analysis. Muscari et al[2] concluded that a main pancreatic duct diameter of 3 mm or less was an independent factor for PF. His group also found that an abundant secretion of pancreatic juice in the soft pancreas increases the risk of PF.[2] The role of octreotide in preventing PF remains controversial, however, and the efficacy of octreotide in established PF is more questionable.[5,6] It thus seems to be very difficult to suppress the secretion of pancreatic juice completely in modern medicine. Success in doing so is expected to be very useful for achieving perfect PJ without PF.

Our group assumed that the best way to achieve 0 PF was to accelerate the healing process of PJ by a novel device during the early postoperative period. We sought to accomplish this by evaluating the healing process of PJ during the early period and the potential cause of anastomotic leakage. Observations by Yonekawa[20] revealed a border zone consisting of a dead space with bloody exudates and migrating inflammatory cells on the 3rd day, followed by the appearance of granulation tissue appeared from the 6th to 7th day. Takami[21] noted a similar migration of fibroblasts with collagen synthesis from the 6th to 7th day, and from the 14th to 30th, they observed a neovascularization that ultimately lead to the completion of the anastomoses. The observations by Yonekawa[20] and Takami[21] on the 3rd to 5th days also revealed anastomotic leakage caused by bacterial infections into the dead space and substantial slowdowns in the formulation of the granulation tissue.[20,21] Our group formed 2 hypotheses: first, that the acceleration of collagen synthesis and neovascularization during the early period was key to preventing PF; second, that granulation tissue formation could be induced during the early period by adopting tissue engineering strategies that enable growth factors to retain their biologic activity. We tried to test these hypotheses by designing an experimental model of PJ using the controlled-released delivery system of bFGF (bFGF-GH).

One important point goal in this study was to select the optimal method for applying bFGF-GH to the anastomotic site of the PJ. Researchers have recently engineered a controlled-release system of GH microspheres incorporating growth factors.[13,14] The growth factors are gradually released as the GH degrades over the course of days or weeks in situ.[13,14] The rate of release can be controlled by modifying the water content of the hydrogels.[13,14] In our study we prepared 100 μg of bFGF-GH with the appropriate water content for complete degradation within 1 week. This modification enabled us to examine the effect of the controlled-release bFGF on day 7. In selecting the shape of the GH, we decided to use a microsphere rather than a sheet or disk (all 3 shapes can be easily processed).[22] We expected that the application of a sheet or disk to the anastomotic site would prevent a close connection between the jejunum and the pancreatic stump. We also wanted to avoid a scattered dispersion of the bFGF-GH over the anastomotic area, as the bFGF would be rapidly diffused from the point of administration and metabolized. Thus, we designed a method of subserosal injection of bFGF-GH into the anastomotic intestine and examined the efficacy of the method in a preliminary study using a rat model. A histologic comparison of bFGF and free-bFGF groups revealed abundant collagen and fibroblasts in the subserosal layer of the former. bFGF-GH has also been found to promote tissue

regeneration more effectively than free bFGF in a model of pressure-induced decubitus ulcer.[23] These results suggest that a subserosal injection of bFGF effectively induces granulation tissue, and that bFGF-GH is a longer-acting and more potent agent than free bFGF.

No anastomotic leakage was observed in the bFGF-GH group. Moreover, all animals survived the surgical procedures without any morbidity in the bFGF-GH group. A close and tightly connected anastomosis between the pancreatic remnant and the jejunum was detected in every animal of the bFGF-GH group even on the 7th day. In contrast, the cohesion between the pancreatic remnant and the intestine separated easily in the control group.

The local application of bFGF-GH induced enormous proliferation of fibroblasts and dense collagen at the anastomotic site in comparison with the control. The incorporation of bFGF-GH into artificial dermis has been reported to accelerate cellular proliferation and connective tissue synthesis in the wound healing of a full-thickness wound.[24] bFGF-GH was even found to induce connective tissue regeneration in a pressure-induced decubitus ulcer in mice with impaired wound healing.[23] Structural collagen determines the early anastomotic strength by providing anchorage to the sutures.[25] Collagen synthesis influences the breaking strength of a healing wound, and the mechanical strength of anastomosis depends on the amount of the structural collagen.[25] The breaking strength of PJ in the bFGF-GH group of our study was significantly higher than that of the control group. These data suggest that bFGF-GH helps to increase the mechanical strength of PJ by accelerating collagen synthesis.

On the other hand, bFGF-GH induced marked formation of new capillaries in the border zone even on 7th day in this model. Kawai et al[23] came to 2 conclusions: first, that bFGF-GH accelerated angiogenesis in the wounds of healing-impaired diabetic mice; second, that bFGF conferred resistance to infection through neovascularization while gradually suppressing wound infection. Angiogenesis at the anastomotic site is therefore crucial for the granulation formation. It also may help to prevent the spread of bacterial infection into the dead space with bloody exudates in the border zone, which is a possible cause of anastomotic leakage.

Additional studies will be required to develop this technique to a level appropriate for use in the clinical setting. The first steps in this direction will be to investigate adequate concentrations of bFGF, the adverse effect of bFGF-GH, and the long-term outcome of the current study. Later we hope to examine whether this technique can reduce the incidence of anastomotic leakage in a model of complicated PF.

In conclusion, bFGF-GH accelerated collagen synthesis and neovascularization in the border zone of pancreaticojejunal anastomosis, whereupon the PJ was completed without anastomotic leakage during the early period. This technique may hold promise for clinical use in the future.

This study was carried out at Nippon Veterinary and Animal Science University. We would like to thank Ms. Otsubo (technician) at Nippon Medical School and Shidow Torisu, DVM, PhD, Yougo Kondo, DVM, PhD, Makoto Washizu, DVM, PhD, and the veterinary students at Nippon Veterinary and Animal Science University.

REFERENCES

1. Shrikhande SV, Qureshi SS, Rajneesh N, Shukla PJ. Pancreatic anastomoses after pancreaticoduodenectomy: do we need further studies? World J Surg 2005;29:1642-9.
2. Muscari F, Suc B, Kirzin S, Hay JM, Fourtanier G, Fingerhut A, et al. Risk factors for mortality and intra-abdominal complications after pancreatoduodenectomy: multivariate analysis in 300 patients. Surgery 2005;139:591-8.
3. Bassi C, Falconi M, Molinari E, Salvia R, Butturini G, Sartori N, et al. Reconstruction by pancreaticojejunostomy versus pancreaticogastrostomy following pancreatectomy. Results of a comparative study. Ann Surg 2005;242:767-73.
4. Duffas JP, Suc B, Msika S, Fourtanier G, Muscari F, Hay JM, et al. A controlled randomized multicenter trial of pancreatogastrostomy or pancreatojejunostomy after pancreatoduodenectomy. Am J Surg 2005;189:720-9.
5. Li-Ling J, Irving M. Somatostatin and octreotide in the prevention of postoperative pancreatic complications and the treatment of enterocutaneous pancreatic fistulas: a systematic review of randomized controlled trials. Br J Surg 2001;88:190-9.
6. Gouillat C, Chpponi J, Baulieux J, Partensky C, Saric J, Gayet B. Randomized controlled multicentre trial of somatostatin infusion after pancreaticoduodenectomy. Br J Surg 2001;88:1456-62.
7. Steenfos HH. Growth factors and wound healing. Scand J Plast Reconst Surg Hand Surg 1994;2:95-105.
8. Nugent MA, Iozzo RV. Fibroblast growth factor-2. Int J Biochem Cell Biol 2000;32:115-20.
9. Buntrock P, Jentzsch KD, Heder G. Stimulation of wound healing, using brain extract with fibroblast growth factor (FGF) activity. I. Quantitative and biochemical studies into formation of granulation tissue. Exp Pathol 1982;21:46.
10. McGee GS, Davidson JM, Buckley A, Sommer A, Woodward SC, Aquino AM, et al. Recombinant basic fibroblast growth factor accelerates wound healing. J Surg Res 1988;45:145.
11. Broadley KN, Aquino AM, Woodward SC, Buckley-Sturrock A, Sato Y, Rifkin DB, et al. Monospecific antibodies implicate basic fibroblast growth factor in normal wound repair. Lab Invest 1989;61:571-5.
12. Steenfos HH, Tarnow P, Aram M, Nakamura T, Jansson J. Increased gene expression of scatter factor-hepatocyte growth factor and basic fibroblast growth factor in granulation tissue in the rat. Wound Repair Regen 1993;1:231-5.
13. Tabata Y. Significance of release technology in tissue engineering. Drug Discov Today 2005;10:1639-46.

14. Tabata Y, Hijikata M, Ikeda Y. Enhanced vascularization and tissue granulation by basic fibroblast growth factor impregnated in gelatin hydrogels. J Control Release 1994;31:189-99.
15. Igai H, Chang SS, Gotoh M, Yamamoto Y, Misaki N, Okamoto T, et al. Regeneration of canine tracheal cartilage by slow release of basic fibroblast growth factor from gelatin sponge. ASAIO J 2006;52:86-91.
16. Grikscheit TC, Siddique A, Ochoa ER, Srinivasan A, Alsberg E, Hodin RA, et al. Tissue-engineered small intestine improves recovery after massive small bowel resection. Ann Surg 2004;240:748-54.
17. Ikeda Y, Tabata Y. Protein release from gelatin matrices. Adv Drug Deliv Rev 1998;31:287-301.
18. Ehrlich HP, Traver H, Hunt TK. Effects of vitamin A and glucocorticoids upon inflammation and collagen synthesis. Ann Surg 1973;177:222-7.
19. Ogawa Y, Chung YS. Microvessel quantitation in invasive breast cancer by staining for factor VII-related antigen. Br J Cancer 1995;71:1297-1301.
20. Yonekawa M. A study of the healing process of pancreaticoenterostomy (in Japanese). J Jpn Surg Soc 1985;86:725-37.
21. Takami H. Studies on the wound healing process of anastomosis of pancreaticojejunostomy using normal and duct ligated pancreas (in Japanese). J Keio Med Soc 1985; 62:629-52.
22. Tabata Y, Hijikata S, Muniruzzaman M, Ikada Y. Neovascularization effect of biodegradable gelatin microspheres incorporating basic fibroblast growth factor. J Biomater Sci Polym Ed 1999;10:79-94.
23. Kawai K, Suzuki S, Tabata Y, Nishimura Y. Accelerated wound healing through the incorporation of basic fibroblast growth factor impregnated gelatin microspheres into artificial dermis using a pressure-induced decubitus ulcer model in genetically diabetic mice. Br J Plast Surg 2005;58:1115-23.
24. Kawai K, Suzuki S, Tabata Y, Ikada Y, Nishimura Y. Accelerated tissue regeneration through incorporation of basic fibroblast growth factor-impregnated gelatin microspheres into artificial dermis. Biomaterials 2000;21: 489-99.
25. Ono I. The effect of basic fibroblast growth factor (bFGF) on the breaking strength of acute incisional wounds. J Dermatol Sci 2002;29:104-13.

Formation of Dentin-like Particles in Dentin Defects above Exposed Pulp by Controlled Release of Fibroblast Growth Factor 2 from Gelatin Hydrogels

Naoki Kikuchi, DDS, Chiaki Kitamura, DDS, PhD,* Takahiko Morotomi, DDS, PhD,* Yoshio Inuyama, DDS,* Hirotaka Ishimatsu, DDS,* Yasuhiko Tabata, PhD, DMedSci, DPharm,† Tatsuji Nishihara, DDS, PhD,‡ and Masamichi Terashita, DDS, PhD**

Abstract

The induction of dentin formation on exposed dental pulp is a major challenge in research on the regeneration of the dentin-pulp complex. We examined the effects of fibroblast growth factor 2 (FGF2), which was delivered in either a collagen sponge (noncontrolled release) or incorporated into gelatin hydrogels (controlled release), on the formation of dentin in exposed rat molar pulps. During the early phase of pulp wound healing, pulp cell proliferation and invasion of vessels into dentin defects above exposed pulp were induced in both groups. In the late phase, the induction of dentin formation was distinctly different between the 2 types of FGF2 release. The noncontrolled release of free FGF2 from collagen sponge induced excessive reparative dentin formation in the residual dental pulp, although dentin defects were not noted. In contrast, controlled release of FGF2 from gelatin hydrogels induced the formation of dentin-like particles with dentin defects above exposed pulp. These results suggest the possibility of a novel therapeutic approach for dentin-pulp complex by controlled release of bioactive FGF2. *(J Endod 2007;33:1198–1202)*

Key Words

Dentin defect, fibroblast growth factor 2, gelatin hydrogels, pulp exposure, regeneration

From the *Division of Pulp Biology, Operative Dentistry, and Endodontics, Department of Cariology and Periodontology, Science of Oral Functions, Kyushu Dental College, Kitakyushu; †Department of Biomaterials, Institute for Frontier Medical Sciences, Kyoto University, Kyoto; and ‡Division of Infections and Molecular Biology, Department of Health Promotion, Science of Health Improvement, Kyushu Dental College, Kitayushu, Japan.

Address requests for reprints to Chiaki Kitamura, DDS, PhD, Division of Pulp Biology, Operative Dentistry, and Endodontics, Department of Cariology and Periodontology, Science of Oral Functions, Kyushu Dental College, 2-6-1 Manazuru, Kokurakita, Kitakyushu 803-8580, Japan. E-mail address: chi-aki-k@kyu-dent.ac.jp.

0099-2399/$0 - see front matter

doi:10.1016/j.joen.2007.07.025

Dental pulp wound healing is triggered in response to exposure to a variety of stimuli such as caries, traumatic injury, and restorative procedures. When dental pulp exposure is slight, direct pulp capping or pulpotomy with calcium hydroxide is frequently used to induce pulp wound healing and preserve residual dental pulp. During pulp wound healing, apoptosis of pulp cells including odontoblasts is initially induced, followed by reparative dentinogenesis (1–4). Reparative dentin is formed by odontoblast-like cells differentiated from pulp cells from the residual dental pulp, resulting in a reduction in dental pulp size and vitality.

When a dentin defect and the resultant exposure of dental pulp tissue reach a critical size, there are no known treatments able to preserve and maintain the vitality of dental pulp, and dentists generally remove the whole dental pulp and treat the case endodontically. It was previously reported that local applications of bioactive molecules such as bone morphogenetic proteins (BMPs) (5, 6) and recombinant fusion ameloblastin (7) to pulp exposure induced appropriate reparative dentin formation. However, there are few studies regarding vital pulp therapy to form new dentin in defects and regenerate the dentin-pulp complex (8, 9).

It was recently reported that a controlled release of fibroblast growth factor 2 (FGF2) induced neovascularization and regeneration of several tissues, including skull bone (10) and periodontal tissues (11). Controlled release of biologically active FGF2 has been achieved by the use of gelatin hydrogels incorporating FGF2 (12, 13), which gradually release FGF2 during in vivo biodegradation (Fig. 1*A*) (14, 15). It is well-known that FGF2 is normally stored in the extracellular matrix, is released by enzymatic degradation of extracellular matrix molecules, and plays a role in physiologic and pathologic conditions (16–18). It was also reported that FGF2 regulates enamel and dentin formation of the tooth germ (19–21).

In the present study, we used gelatin hydrogels as a carrier for FGF2 and collagen sponges as a scaffold and examined effects of a controlled release of FGF2 from the gelatin hydrogels on exposed pulp.

Materials and Methods

Preparation of Gelatin Hydrogels Incorporating FGF2

Gelatin hydrogel microspheres (the water content was 95 vol%; diameters ranged from 5–15 μm; the average of diameter was 10 μm) were prepared with gelatin (isoelectric point, 5.0) (Nitta Gelatin, Osaka, Japan) through glutaraldehyde cross-linking of a gelatin solution in an emulsion state. Briefly, 25 μL of glutaraldehyde was immediately mixed with 10 mL of gelatin solution preheated at 40°C. The mixed solution was added dropwise to 375 mL of olive oil while stirring at 420 rpm at 40°C, with the stirring continued for 24 hours at 25°C. After addition of 100 mL of acetone, the resulting microspheres were collected by centrifugation at 3000 rpm at 4°C for 5 minutes, washed by centrifugation, and placed in 100 mL of 100 mmol/L glycine solution containing 0.1% Tween 80, followed by agitation at 37°C for 1 hour to block residual aldehyde groups of unreacted glutaraldehyde. Cross-linked microspheres (av-

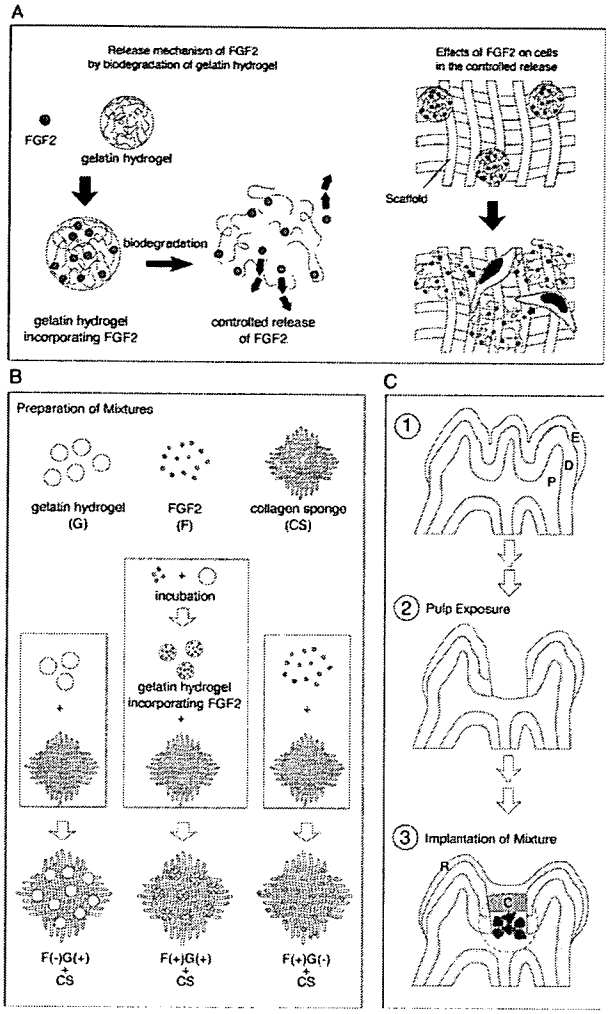

Figure 1. *(A)* Release mechanism of FGF2 from gelatin hydrogels. FGF2 was gradually released from gelatin hydrogels by the biodegradation of gelatin hydrogels. Controlled release of bioactive FGF2 shows continuous effects on cells that invade and proliferate on a scaffold. *(B)* Preparation of mixtures of collagen sponges with FGF2-free gelatin hydrogel microspheres, gelatin hydrogel microspheres incorporating FGF2, and free FGF2. *(C)* Implantation of mixtures into dentin defect above exposed dental pulp. The field from the exposed surface area of dental pulp to dentin defect area in which mixtures were implanted (dotted circle) in each molar was examined histologically and immunohistologically.

erage of diameter, 10 μm) were washed with double-distilled water, freeze-dried, and sterilized with ethylene oxide gas.

Mixtures of collagen sponge with gelatin hydrogel microspheres and FGF2 were prepared just before implantation (Fig. 1*B*). Twenty μL of human recombinant FGF2 (provided by Kaken Pharmaceutical Co, Tokyo, Japan) in phosphate-buffered saline (PBS) (5 μg/μL) was dropped onto 2 mg of freeze-dried gelatin hydrogel microspheres and then left to stand at 4°C for 8 hours to allow impregnation of FGF2 into microspheres. Microspheres incorporating FGF2 were mixed with small pieces of collagen sponge torn by using fine forceps.

Preparation of Rat Molars and Implantation of Mixture

The animal protocol was carried out according to the guidelines for animal care of Kyushu Dental College, with ethical approval obtained from the institutional panel for animal care. Sixty (4 for each experimental group) Wistar specific pathogen-free rats (9-weeks-old), weighing 250–350 g, were maintained under barrier system condition. Fig. 1*C* illustrates the protocol for the study. Rats were deeply anesthetized by intraperitoneal injection of 5% pentobarbital sodium (Nembutal; Dainippon Pharmaceutical Co, Suita, Japan) at a dose of 30 mg/kg, after which the dental pulp was exposed on occlusal aspects of maxillary first molars with a No. 1/2 round bur. After irrigation with a solution of 10% sodium hypochlorite, 3% hydrogen peroxide, and saline, it was dried with paper points; then the mixture of collagen sponge with gelatin hydrogel microspheres incorporating FGF2 (final concentration, 700 ng/μL) was implanted into exposed pulp and capped with α-TCP cement (New apatite liner; DENTSPLY-Sankin KK, Tokyo, Japan). As a control, the mixture of collagen sponge with FGF2-free gelatin hydrogel microspheres was implanted, and the mixture of collagen sponge with free FGF2 (final concentration, 700 ng/μL of PBS) was also implanted as a control for noncontrolled release of free FGF2. To avoid marginal leakage, implanted molars were covered with adhesive resin (Super-Bond C&B; Sun Medical Co, Siga, Japan), and cusps of mandiblar first molars were removed.

Postoperative time intervals of death were 1, 3, 7, 14, and 21 days after surgery. At each interval, rats were anesthetized and killed by transcardial vital perfusion with 4% paraformaldehyde–phosphate buffer, pH 7.3 (4% PFA). Maxillary segments including first molars were carefully dissected and immersed in 4% PFA at 4°C overnight for further fixation. After fixation, first molars were dissected from maxillary segments and demineralized in Microscopy OSTEOSOFT (Merck KGaA, Damstadt, Germany) at 4°C for 4 days. Demineralized molars were dehydrated with graded ethanol and embedded in paraffin. Serial 6-μm sections were cut, mounted on 3-aminopropyltriethoxysilane–treated object slides, and stained with hematoxylin-eosin for histologic analysis.

Immunohistochemistry

Demineralized molars were also immersed in TISSUE-TEK OCT compound (Miles Inc, Elkhart, IN) and frozen in isopentane cooled in solid CO_2. Frozen tissue sections (7-μm thickness) were cut with a cryostat (LEICA Instruments GmbH, Nussloch, Germany). Immunohistochemistry was carried out by using an avidin-biotin-peroxidase complex method with VECTASTAIN ABC kit (Vector Laboratories, Inc, Burlingame, CA). Sections were rinsed with PBS, immersed in 0.3% H_2O_2/methanol, blocked with normal serum solution, and reacted with the primary antibody at 4°C overnight. Goat polyclonal antibody against dentin sialoprotein (DSP) (Santa Cruz Biotechnology, Santa Cruz, CA) was used as the primary antibody at a dilution of 1:100 in PBS. Sections were incubated with biotinylated antibodies for 30 minutes at room temperature and treated with a peroxidase substrate solution containing diaminobenzidine (DAB) (1 mg/mL), Tris/HCl, pH 7.5, and 0.02% H_2O_2. After counterstaining with methyl green (Vector Laboratories, Inc), DAB signals were observed under the light microscopy. Negative controls for DSP were carried out by omitting primary antibody or with nonspecific immunoglobulin G.

Statistical Analysis

We selected 4 serial sections from each molar (4 rats for each group) and used them for semiquantitative analyses. These sections included dentin defects, implanted mixtures, and exposed pulp, which were located at the buccolingual center of the molar (Fig. 1*C-3*). By using Image J (National Institutes of Health, Bethesda, MD), we counted the number of all detectable vessels in pulp tissue that had invaded into implanted mixtures and clearly showed the luminal structure and analyzed the differences in results on the basis of the number of days after implantation by one-way analysis of variance (ANOVA). We also calculated the ratio of all detectable calcified particles to dentin defect area in

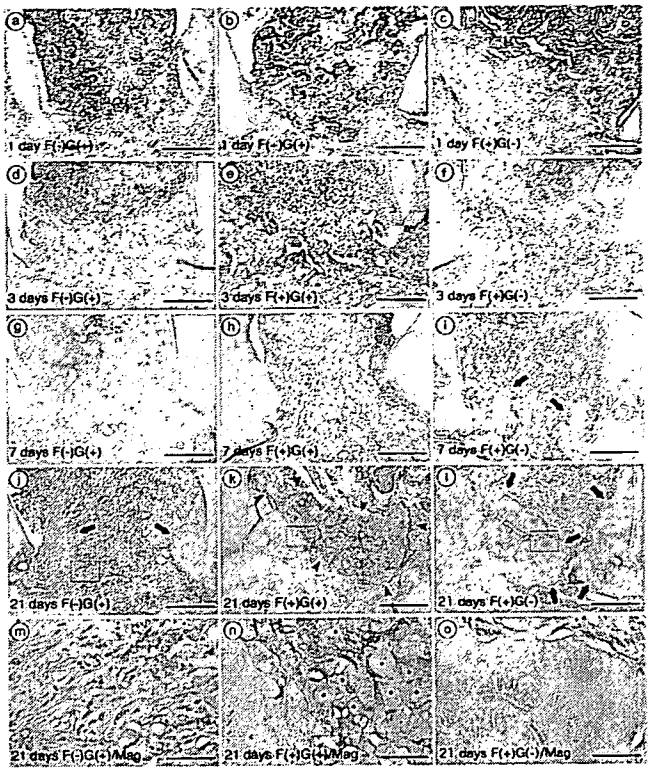

Figure 2. Histologic changes of dentin/pulp complex at 1 day (*a–c*), 3 days (*d–f*), 7 days (*g–i*), and 21 days (*j–o*) after implantation of mixtures. High magnification microphotographs of results after 21 days (rectangular areas in *j–l*) are shown in *m–o*. F(−)G(+), F(+)G(+), and F(+)G(−) refer to implanted mixtures of collagen sponges with FGF2-free gelatin hydrogel microspheres, gelatin hydrogel microspheres incorporating FGF2, and free FGF2, respectively. White arrowheads (*a–c*) indicate collagen sponges. Arrows (*i, j, l*) indicate reparative dentin, whereas black arrowheads (*k*) show the formation of calcified particles, and asterisks (*n*) show calcified particles. F, FGF2; G, gelatin hydrogel microspheres. Scale bars = 100 μm (*a–l*) and 20 μm (*m–o*). Magnification level, 400× (*a–l*) and 1000× (*m–o*).

the group implanted with mixture of collagen sponge with gelatin hydrogel microspheres incorporating FGF2 at 7, 14, and 21 days after surgery by means of Image J. Differences between variables shown by ANOVA were compared with Student *t* tests. All data are expressed as the mean ± standard deviation.

Results

Histologic Changes of Exposed Pulp

One day after surgery, the exposed pulps displayed intimate contact with the treatments (Fig. 2*a–c*) and the local ingrowth of dental pulp cells, and vessels into the mixtures were observed at 3 days (Fig. 2*d–f*). In these early phases (1 and 3 days), there were no differences among 3 groups. Seven days after surgery, the dentin defects in all groups were filled with pulp tissue including vessels, and collagen sponges, which were observed 1 day after surgery, disappeared by biodegradation (Figs 2*g–i*). The initiation of reparative dentin formation was observed in the group implanted with mixture of collagen sponges with free FGF2 (Fig. 2*i*). Twenty-one days after implantation of collagen sponges without FGF2, dentin defects remained to be filled with pulp tissue, and initiation of reparative dentin formation was observed (Fig. 2*j*). Excessive formation of reparative dentin toward residual pulp was observed in the group in which free FGF2 was released (Fig. 2*l, o*). In the group with implanted gelatin hydrogel microspheres incorporating FGF2, we observed eosin-stained calcified particles (Fig. 2*k*). Various sizes of calcified particles (Fig. 2*n*) were found in dentin defect area above exposed pulp, but they were not found in other 2 groups.

Fig. 3*A* shows the numbers of all vessels clearly showing luminal structure in dental pulp proliferating into dentin defects. Numbers of vessels in each group increased from 1 day and peaked at 14 days, after which they decreased at 21 days. Fig. 3*B* shows the ratio of calcified particles to dentin defect area in 3 groups. Calcified particles were found only in the group implanted with gelatin hydrogel microspheres incorporating FGF2, and the ratio of calcified particles to dentin defect area in this group significantly increased in 21 days ($P < .01$).

Expression of DSP During Formation of Calcified Particles

To determine whether the calcified particles observed at 21 days were dentin-like, we analyzed the expression of DSP in pulp cells around calcified particles (Fig. 4*A*). DSP signals were observed sporadically in groups without FGF2 (Fig. 4*A-a*) and with free FGF2 (Fig. 4*A-c*). In contrast, in the group implanted with gelatin hydrogel microspheres incorporating FGF2, intense DSP signals were observed in pulp cells and calcified particles (Fig. 4*A-b*, 4*B-a, b*). In these experiments, negative controls showed no signals of DSP (Fig. 4*B-c*).

Discussion

A number of studies have used FGF2 as a morphogen to induce tissue regeneration (22, 23). However, transient application of FGF2 is a major problem impeding its use for successful tissue regeneration. Recently, it was demonstrated in vivo and in vitro assay that gelatin hydrogels are able to gradually release bioactive FGF2 during their biodegradation and prolong the supply of FGF2 much longer than that observed with the injection of free FGF2 (14, 15). In the present study,

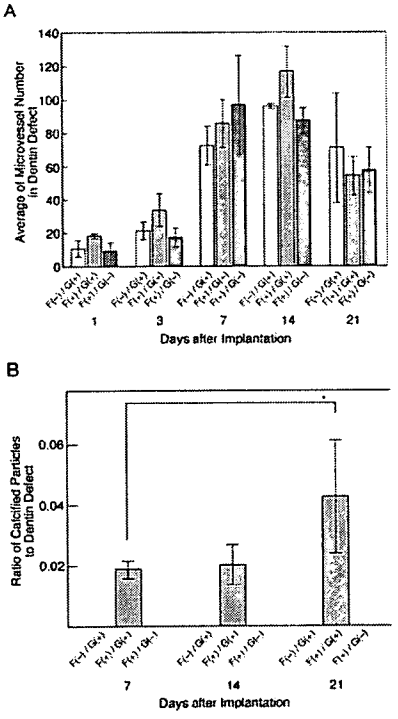

Figure 3. (*A*) The number of vessels in dental pulp tissue proliferating into dentin defect. (*B*) The ratio of calcified particles to dentin defect area in 3 groups. F(−)G(+), F(+)G(+), and F(+)G(−) refer to implanted mixtures of collagen sponges with FGF2-free gelatin hydrogel microspheres, gelatin hydrogel microspheres incorporating FGF2, and free FGF2, respectively. All data are expressed as the mean ± standard deviation. *$P < .01$ (Student *t* test).

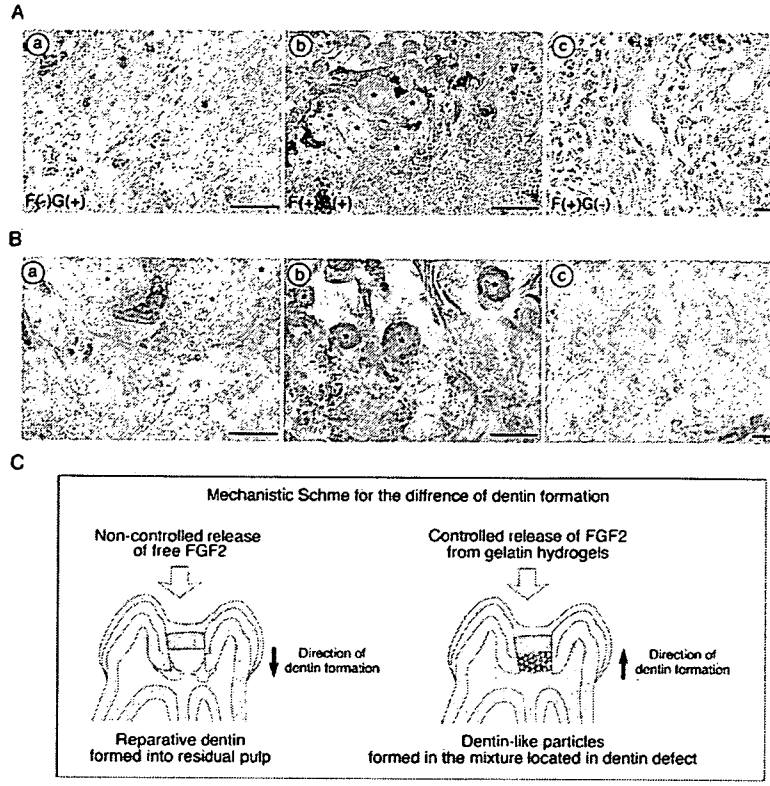

Figure 4. (*A*) Expression of DSP in pulp cells and calcified particles at 21 days. Implanted mixtures were collagen sponges with FGF2-free microspheres (*a*), gelatin hydrogel microspheres incorporating FGF2 (*b*), and free FGF2 (*c*), respectively. Asterisks in (*b*) show calcified particles. F, FGF2; G, gelatin hydrogel microspheres. Scale bars = 20 μm. Magnification level, 400×. (*B*) High magnification of calcified particles and pulp cells expressing DSP (*a, b*) and negative control (*c*). Scale bars = 10 μm. Magnification level, 1000×. (*C*) Mechanistic scheme about reparative dentin formation toward residual pulp by noncontrolled release of free FGF2 and the formation of dentin-like particles in dentin defects by controlled release of FGF2.

we used gelatin hydrogels incorporating FGF2 on exposed pulp and compared effects of controlled release of FGF2 on the induction of new dentin formation with noncontrolled release of free FGF2 from collagen sponge.

During the early phase of pulp wound healing, the invasion of vessels and proliferation of pulp cells into dentin defects were induced in all groups, although FGF2 showed a tendency to accelerate invasion. In the late phase, however, we found distinct effects of controlled release of FGF2 from gelatin hydrogels with regards to new dentin formation. Gelatin hydrogels without FGF2 did not accelerate dentin formation both in residual pulp and in dentin defects above exposed pulp, suggesting that gelatin hydrogels do not affect the process of reparative dentin formation during wound healing of exposed pulp. Noncontrolled release of free FGF2 from collagen sponges only induced excessive reparative dentin formation toward residual dental pulp, not in dentin defects above exposed pulp, suggesting that noncontrolled release of free FGF2 might accelerate reparative dentin formation. In contrast, controlled release of FGF2 induced the formation of calcified particles in dentin defects. Those calcified particles as well as pulp cells around the particles expressed DSP, one of the markers of odontoblasts and odontoblast-like cells in dental pulp. Several studies have demonstrated the proliferation and DSP expression of pulp cells by FGF2 (24) and the existence of pulp stem cells that have the ability to differentiate into odontoblast-like cells expressing DSP (25). Our results might suggest that controlled release of FGF2 induces differentiation of proliferating pulp stem cells to odontoblast-like cells in the collagen sponge, and that calcified particles in dentin defects are dentin-like structures formed by odontoblast-like cells.

The ideal means to regenerate dentin is to induce a nonporous, tubular, dentin-like structure similar to natural sound dentin. In the present study, the induced dentin in defect areas was a porous aggregate composed of dentin-like particles. The imperfection of the regenerated dentin might have been due to the dose of FGF2 incorporated into gelatin hydrogels, or because other bioactive molecules such as BMPs were not added. We are continuing research to clarify the appropriate FGF2 dosage and the combination of other molecules for induction of nonporous new dentin before clinical applications.

The induction of dentin formation into dentin defect as well as pulp cells is essential for the regeneration of dentin-pulp complex (26, 27). We show that the release modality of FGF2 applied to exposed pulp affects the induction of new dentin formation (Fig. 4*C*). Noncontrolled release of FGF2 only accelerates reparative dentin formation in residual dental pulp, whereas controlled release of FGF2 induces the formation of dentin-like particles in dentin defects above exposed pulp, suggesting the possibility of a novel therapeutic approach for dentin-pulp complex.

Acknowledgments

This research was supported by Grants in Aid for Scientific Research 18592094 and 18209057 (C.K.) from The Ministry of Education, Science, and Culture of Japan, Tokyo, Japan.

References

1. Kitamura C, Ogawa Y, Nishihara T, Morotomi T, Terashita M. Transient co-localization of c-Jun N-terminal kinase and c-Jun with heat shock protein 70 in pulp cells during apoptosis. J Dent Res 2003;82:91–5.

2. Kitamura C, Nishihara T, Ueno Y, Nagayoshi M, Kasugai S, Terashita M. Thermotolerance of pulp cells and phagocytosis of apoptotic pulp cells by surviving pulp cells following heat stress. J Cell Biochem 2005;94:826–34.
3. Kitamura C, Nishihara T, Ueno Y, et al. Effects of sequential exposure to lipopolysaccharide and heat stress on dental pulp cells. J Cell Biochem 2006;99:797–806.
4. Ueno Y, Kitamura C, Terashita M, Nishihara T. Reoxygenation improves hypoxia induced pulp cell arrest. J Dent Res 2006;85:824–8.
5. Rutherford RB, Gu K. Treatment of inflamed ferret dental pulps with recombinant bone morphogenetic protein-7. Eur J Oral Sci 2000;108:202–6.
6. Six N, Lasfargues JJ, Goldberg M. Differential repair responses in the coronal and radicular areas of the exposed rat molar pulp induced by recombinant human bone morphogenetic protein 7 (osteogenic protein 1). Arch Oral Biol 2002;47:177–87.
7. Nakamura Y, Slaby I, Spahr A, Pezeshki G, Matsumoto K, Lyngstadaas SP. Ameloblastin fusion protein enhances pulpal healing and dentin formation in porcine teeth. Calcif Tissue Int 2006;78:278–84.
8. Nakashima M. Induction of dentin formation on canine amputated pulp by recombinant human bone morphogenetic protein (BMP)-2 and -4. J Dent Res 1994;73:1515–22.
9. Nakashima M, Tachibana K, Iohara K, Ito M, Ishikawa M, Akamine A. Induction of reparative dentin formation by ultrasound-mediated gene delivery of growth/differentiation factor 11. Hum Gene Ther 2003;14:591–7.
10. Tabata Y, Yamada K, Hong L, Miyamoto S, Hashimoto N, Ikada Y. Skull bone regeneration in primates in response to basic fibroblast growth factor. J Neurosurg 1999;91:851–6.
11. Nakahara T, Nakamura T, Kobayashi E, et al. Novel approach to regeneration of periodontal tissues based on in situ tissue engineering: effects of controlled release of basic fibroblast growth factor from a sandwich membrane. Tissue Eng 2003;9:153–62.
12. Tabata Y, Ikada Y. Vascularization effect of basic fibroblast growth factor released from gelatin hydrogels with different biodegradabilities. Biomaterials 1999; 20:2169–75.
13. Tabata Y, Miyano M, Inamoto T, et al. De novo formation of adipose tissue by controlled release of basic fibroblast growth factor. Tissue Eng 2000;6:279–89.
14. Tabata Y, Nagano A, Ikada Y. Biodegradation of hydrogel carrier incorporating fibroblast growth factor. Tissue Eng 1999;5:127–38.
15. Yamamoto M, Ikada Y, Tabata Y. Controlled release of growth factors based on biodegradation of gelatin hydrogel. J Biomater Sci Polym Ed 2001;12:77–88.
16. Annabi B, Naud E, Lee YT, Eliopoulos N, Galipeau J. Vascular progenitors derived from murine bone marrow stromal cells are regulated by fibroblast growth factor and are avidly recruited by vascularizing tumors. J Cell Biochem 2004;91:1146–58.
17. Etscheid M, Beer N, Kress JA, Seitz R, Dodt J. Inhibition of bFGF/EGF-dependent endothelial cell proliferation by the hyaluronan-binding protease from human plasma. Eur J Cell Biol 2004;82:597–604.
18. Taylor KR, Rudisill JA, Gallo RL. Structural and sequence motifs in dermatan sulfate for promoting fibroblast growth factor-2 (FGF-2) and FGF-7 activity. J Biol Chem 2005;280:5300–6.
19. Tsuboi T, Mizutani S, Nakano M, Hirukawa K, Togari A. Fgf-2 regulates enamel and dentine formation in mouse tooth germ. Calcif Tissue Int 2003;73:496–501.
20. Madan AK, Kramer B. Immunolocalization of fibroblast growth factor-2 (FGF-2) in the developing root and supporting structures of the murine tooth. J Mol Histol 2005;36:171–8.
21. Tran-Hung L, Mathieu S, About I. Role of human pulp fibroblasts in angiogenesis. J Dent Res 2006;85:819–23.
22. Nagai H, Tsukuda R, Mayahara H. Effects of basic fibroblast growth factor (bFGF) on bone formation in growing rats. Bone 1995;16:367–73.
23. Kato T, Kawaguchi H, Hanada K, et al. Single local injection of recombinant fibroblast growth factor-2 stimulates healing of segmental bone defects in rabbits. J Orthop Res 1998;16:654–9.
24. Nakao K, Itoh M, Tomita Y, Tomooka Y, Tsuji T. FGF-2 potently induces both proliferation and DSP expression in collagen type I gel cultures of adult incisor immature pulp cells. Biochem Biophys Res Comm 2004;325:1052–9.
25. Gronthos S, Mankani M, Brahim J, Robey PG, Shi S. Postnatal human dental pulp stem cells (DPSCs) in vitro and in vivo. Proc Natl Acad Sci USA 2000;97:13625–30.
26. Murray PE, Garcia-Godoy F, Hargreaves KM. Regenerative endodontics: a review of current status and a call for action. J Endod 2007;33:377–90.
27. Nakashima M, Akamine A. The application of tissue engineering to regeneration of pulp and dentin in endodontics. J Endod 2005;31:711–8.